Stellar substructures in the solar neighbourhood

IV. Kinematic Group 1 in the Geneva-Copenhagen survey

R. Ž+enovienė[1], G. Tautvaišienė[1], B. Nordström[2,3], E. Stonkutė[1], and G. Barisevičius[1]

[1] Institute of Theoretical Physics and Astronomy, Vilnius University, A. Gostauto 12, 01108 Vilnius, Lithuania
e-mail: [renata.zenoviene;grazina.tautvaisiene;edita.stonkute;gintaras.barisevicius]@tfai.vu.lt
[2] Dark Cosmology Centre, Niels Bohr Institute, Copenhagen University, Juliane Maries Vej 30, DK-2100, Copenhagen, Denmark
[3] Stellar Astrophysics Centre, Department of Physics and Astronomy, Aarhus University, Ny Munkegade 120, DK-8000 Aarhus C, Denmark
e-mail: birgitta@nbi.ku.dk

ABSTRACT

Context. A combined study of kinematics and chemical composition of stars is one of the most promising tools of research in Galaxy formation. The main goal in this field of research is to reconstruct the formation history of our Galaxy, to reveal the origin of the thick disc, and to find remnants of ancient mergers.

Aims. We determine detailed elemental abundances in stars belonging to the so-called Group 1 of the Geneva-Copenhagen survey (GCS) and compare the chemical composition with the Galactic thin- and thick-disc stars, with the GCS Group 2 and Group 3 stars, as well as with several kinematic streams of similar metallicities. The aim is to search for chemical signatures that might give information about the formation history of this kinematic group of stars.

Methods. High-resolution spectra were obtained with the Fibre-fed Echelle Spectrograph (FIES) spectrograph at the Nordic Optical Telescope, La Palma, and were analysed with a differential model atmosphere method. Comparison stars were observed and analysed with the same method.

Results. The average value of [Fe/H] for the 37 stars of Group 1 is -0.20 ± 0.14 dex. Investigated Group 1 stars can be separated into three age subgroups. Along with the main 8- and 12-Gyr-old populations, a subgroup of stars younger than 5 Gyr can be separated as well. Abundances of oxygen, α-elements, and r-process dominated elements are higher than in Galactic thin-disc dwarfs. This elemental abundance pattern has similar characteristics to that of the Galactic thick disc and differs slightly from those in Hercules, Arcturus, and AF06 stellar streams.

Conclusions. The similar chemical composition of stars in Group 1, as well as in Group 2 and 3, with that in stars of the thick disc might suggest that their formation histories are linked. The chemical composition pattern together with the kinematic properties and ages of stars in the investigated GCS groups provide evidence of their common origin and possible relation to an ancient merging event. A gas-rich satellite merger scenario is proposed as the most likely origin.

Key words. stars: abundances – Galaxy: disc – Galaxy: formation – Galaxy: evolution

1. Introduction

In this series of papers (Stonkutė et al. 2012, 2013, hereafter Paper I and Paper II; and Ž+enovienė et al. 2014, hereafter Paper III), we investigate the detailed chemical composition of stellar kinematic groups that were identified in the Geneva-Copenhagen survey (GCS, Nordström et al. 2004) and were suggested to belong to remnants of ancient merger events in our Galaxy (Helmi et al. 2006).

The formation and evolution of the Milky Way galaxy is one of the greatest outstanding questions of astrophysics. According to Lambda cold dark matter (ΛCDM) cosmological model, large galaxies like our Galaxy emerge as an end-point of hierarchical clustering, merging, and accretion, but we still lack the detailed physical picture of how individual stellar populations can be associated with elements of the proto-cloud, and how different Galactic components formed and evolved. Even the thick disc, as a unique Galactic component discovered more than 30 years ago (Gilmore & Reid 1983), still has no approved formation scenario. Separation of the Galactic disc into "thick" and "thin" disc populations refers to different types of stars. Thick-disc stars are

essentially older and more highly enriched in α-elements than thin-disc stars (e.g. Soubiran & Girard 2005). The enhancement in α-elements suggests that the thick-disc stars were formed on relatively short timescales (~ 1 Gyr), thus offering us a hint to the formation history of our Galaxy (Kordopatis et al. 2013a). Ancient minor mergers of satellite galaxies are considered as one possible scenario of the thick-disc formation.

Numerical simulations of merger events have shown that such debris streams survive as coherent structures over gigayears (Helmi 2004; Law et al. 2005; Peñarrubia et al. 2005). Stellar streams may be discovered as overdensities in the phase space distribution of stars in the solar vicinity. Examining the GCS catalogue, Helmi et al. (2006) looked for stellar streams in a space of orbital apocentre, pericentre, and z-angular momentum (L_z), the so-called APL-space. In this kind of space stellar streams cluster around lines of constant eccentricity. They found three new coherent stellar groups (Group 1, 2, and 3) with distinctive ages, metallicities, and kinematics, and suggested that those groups might correspond to remains of disrupted satellites.

Arifyanto & Fuchs (2006), Dettbarn et al. (2007), and Klement et al. (2008) proposed an alternative projection of the

eccentricity and L_z space, which according to Dekker's (1976) theory of Galactic orbits can be approximated by $(U^2 + 2V^2)^{1/2}$ and V velocities, respectively (U is pointing towards the Galactic center, V into the direction of Galactic rotation). The assumption is that stars in the same stellar stream move on orbits that stay close together, which is justified by numerical simulations of satellite disruptions (Helmi et al. 2006). With this method, Arifyanto & Fuchs (2006) identified several known streams (Hyades-Pleiades, Hercules, and Arcturus) and one new, the so-called AF06 stream (later confirmed by Klement et al. 2009 and by Klement et al. 2011).

Dettbarn et al. (2007) analysed the phase space distribution in a sample of non-kinematically selected low metallicity stars in the solar vicinity and determined the orbital parameters of several halo streams. One of those streams seemed to have precisely the same kinematics as the Sagittarius stream.

Klement et al. (2008) searched for stellar streams or moving groups in the solar neighbourhood, using data provided by the first RAVE public data release. They estimated overdensities related to the Sirius, Hercules, Arcturus, and Hyades-Pleiades moving groups. Besides, they found a new stream candidate (KFR08), suggesting that its origin is external to the Milky Way's disc. The KFR08 stream later was confirmed by Klement et al. (2009) and Bobylev et al. (2010). Antoja et al. (2012) also used the RAVE data and discovered a new group at $(U, V) = (92, -22)\,\mathrm{km\,s^{-1}}$ in the solar neighbourhood. The new group was detected as a significant overdensity in the velocity distributions using a technique based on the wavelet transform.

A mechanism, known as 'ringing' was introduced by Minchev et al. (2009). Minchev et al. (2009) showed that the sudden energy kick imparted by the gravitational potential of the satellite as it crosses the plane of the disc can strongly perturb the velocity field of disc stars located in local volumes such as the solar neighbourhood. These perturbations can be observed in the (U, V) plane as arc-like features travelling in the direction of positive V (see Gómez et al. 2012). Using this technique Minchev et al. (2009) confirmed presence of several known moving groups and predicted four new features at $V \sim -140, -120, 40, 60\,\mathrm{km\,s^{-1}}$. By matching the number and positions of the observed streams, they estimated that the Milky Way disc was strongly perturbed about 1.9 Gyr ago.

Various studies have been searching for evidence of minor-merger events in the Milky Way (see review by Klement 2010). Large and deep chemodynamical surveys such as *Gaia* (Perryman et al. 2001) will enable us to characterise the Galaxy more precisely and to examine its formation scenarios as well as the kinematic stellar group identification methods.

An indispensable method to check the origin of various kinematic streams is the investigation of their chemical composition. In this paper, we present the detailed chemical composition of stars belonging to Group 1 of the Geneva-Copenhagen survey, which was identified by Helmi et al. (2006).

High-resolution spectra of 21 stars in the most metal-deficient GCS Group 3 were investigated in Paper I and Paper II. Paper III presented results of the analysis of 32 stars in the GCS Group 2. Galactic thin-disc stars were analysed for a comparison as well. We present the detailed chemical composition results for Group 1, the last group of GCS. This kinematic group, which is the most numerous and metal-rich among the GCS groups, consists of 120 stars. According to the (Nordström et al. 2004) catalogue, its mean photometric metallicity, [Fe/H], is about -0.45 dex. The Group 1 stars are distributed into two age populations of 8 Gyr and 12 Gyr. Group 1 also differs from the other two groups by different metallicity and kinematics, and tends

to have a significantly smaller z-velocity dispersion. We investigated chemical composition for 37 Group 1 stars, eight comparison Galactic thin-disc stars, and five comparison Galactic thick-disc stars. We determined abundances of up to 22 chemical elements and compared them with the Galactic disc abundance pattern.

In Fig. 1, we show the velocity distribution of the Galactic disc stars from Holmberg et al. (2009). Stars belonging to GCS Group 1 are marked with open and filled circles (the latter are used to mark stars we investigated). An average error of stellar space motions in each component (U, V, and W) is 1.5 $\mathrm{km\,s^{-1}}$ (Nordström et al. 2004). It is clear from Fig. 1 that the distribution of Group 1 stars in the velocity space differs in comparison to other stars of the Galactic disc. For example in the (U, V) plane Group 1 stars are distributed in a banana shape, whereas the thin-disc stars define a centrally concentrated clump. These characteristic patterns are the same as those of infalling dwarf satellites after several gigayears (see Helmi et al. 2006 for a comprehensive discussion). In Fig. 2, the stars are shown in the APL-space. Kinematic group stars spread out in the edge of the distribution of data points. The location of a star in the APL space is very accurate. A limited knowledge of the form of the Galactic potential, used to determine values of apocentre and pericentre, does not affect the distribution of points in the APL space much because the volume probed by the GCS sample is so small that the Galactic potential is close to a constant inside this region (c.f. Helmi et al. 2006). This implies that the energy, and hence the orbital parameters or the location of a star in the APL space, are determined mostly by its kinematics rather than by its spatial location (or the Galactic potential). Changes in the Galactic potential produce only small variations in the orbital parameters. According to Helmi et al. (2006), in the case of the potential proposed by Flynn et al. (1996), which was used for the orbit integrations in Nordström et al. (2004) and the following papers, a typical change in the apocentre and pericentre is of about 1–2 %.

Despite the fact that the kinematic group members, over time, were dispersed through the Galactic disc, their chemical composition should remain unchanged. The high-resolution spectroscopic analysis is an important supplemental method in revealing and confirming the origin and history of the GCS stellar groups.

2. Observations and analysis

We obtained high-resolution spectra of the programme and comparison stars with the Fibre-fed Echelle Spectrograph on the Nordic Optical 2.5 m telescope (NOT) during 2008, 2011, and 2012. This spectrograph gives spectra of resolving power ($R \approx 68\,000$) in the wavelength range of 3680–7270 Å. We exposed the spectra to reach a signal-to-noise ratio higher than 100. We elected the programme stars so that they were observable from the NOT and were brighter than $V = 10$ mag. Reductions of CCD images were made with the FIES pipeline *FIEStool*, which performs a complete reduction: calculation of reference frame, bias and scattering subtraction, flat-field division, wavelength calibration and other procedures (http://www.not.iac.es/instruments/fies/fiestool). A list of the observed stars and some of their parameters (taken from the catalogue of Holmberg et al. 2009 and SIMBAD) are presented in Table 1.

We analysed the spectra using the differential model atmosphere technique described in Papers I, II, and III. Here we will revisit only a few details. The Eqwidth and BSYN program packages, developed at the Uppsala Astronomical
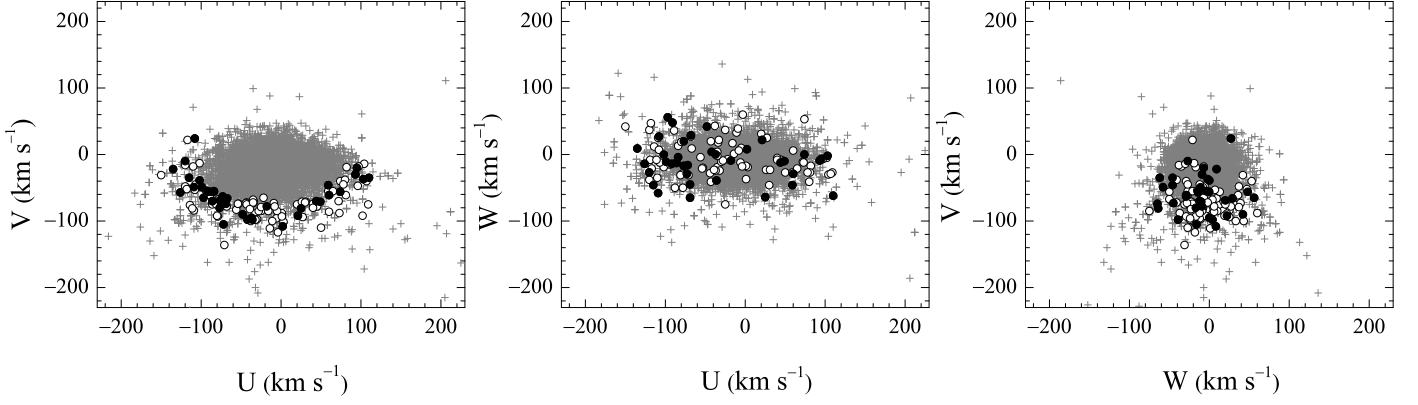
Fig. 1. Velocity distribution for all stars in the sample of Holmberg et al. (2009) (plus signs), stars of Group 1 (circles), and the stars investigated here (filled circles).
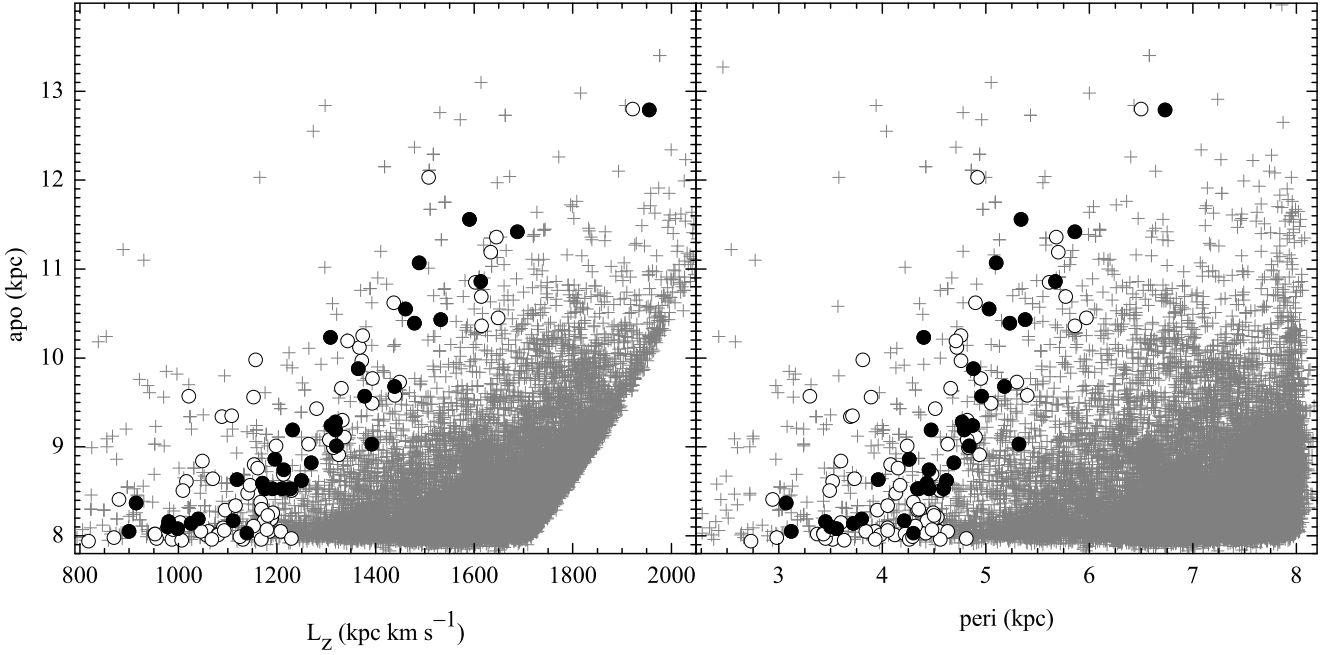

Fig. 2. Distribution for the stars in the APL space. Plus signs denote the GCS sample (Holmberg et al. 2009), circles denote Group 1, the filled circles are the stars we investigated. Note that these stars as well as all Group 1 stars are distributed in APL space with constant eccentricity.

Observatory, were used to carry out the calculation of abundances from measured equivalent widths and synthetic spectra, respectively. A set of plane-parallel, line-blanketed, constant-flux LTE model atmospheres (Gustafsson et al. 2008) were taken from the MARCS stellar model atmosphere and flux library (http://marcs.astro.uu.se/).

We used the Vienna Atomic Line Data Base (VALD, Piskunov et al. 1995) to prepare input data for the calculations. We took the atomic oscillator strengths for the main spectral lines we analysed from an inverse solar spectrum analysis performed in Kiev (Gurtovenko & Kostyk 1989).

Initial values of the effective temperatures for the programme stars were taken from Holmberg et al. (2009) and then carefully checked and corrected, if needed, by forcing Fe ı lines to yield no dependency of iron abundance on excitation potential through changes to the model effective temperature. We used the ionisation equilibrium method to find surface gravities of the programme stars by forcing neutral and ionised iron lines to yield the same iron abundances. Microturbulence velocity values cor-

responding to the minimal line-to-line Fe ı abundance scattering were chosen as correct values. We performed the spectral synthesis method for the determination of oxygen, yttrium, zirconium, barium, lanthanum, cerium, praseodymium, neodymium, samarium, and europium abundances. Several fits of the synthetic line profiles to the observed spectra are shown in Figs. 5–8. We complied atomic parameters of lines in the intervals of spectral syntheses from the VALD database. We calibrated all log *gf* values to fit to the solar spectrum by Kurucz (2005) with solar abundances from Grevesse & Sauval (2000). We took hyperfine structures and isotope shifts into account as appropriate. Abundances of other chemical elements were determined using equivalent widths of their lines. We determined abundances of Na and Mg taking non-local thermodynamical equilibrium (NLTE) into account. The equivalent widths of the lines were measured by fitting of a Gaussian profile using the 4A software package (Ilyin 2000).

The uncertainties in abundances are due to several sources: uncertainties caused by analysis of individual lines, including

Table 1. Parameters of programme and comparison stars

Star	Sp. type	Age H09[*]	Age C11[*]	M_V mag	d pc	U km s^{-1}	V km s^{-1}	W km s^{-1}	e	z_{max} kpc	R_{peri} kpc	R_{apo} kpc
					Group 1 stars							
HD 3795	K0V	10.6	9.9	3.84	29	-48	-90	42	0.37	1.07	3.80	8.19
HD 4607	F5	4.2	3.5	3.08	85	-108	24	27	0.31	0.86	6.73	12.79
HD 15777	G0	11	11.1	4.28	50	-77	-69	20	0.32	0.50	4.45	8.74
HD 22872	F9V	6.2	5.9	3.59	74	-99	-49	-11	0.32	0.06	4.96	9.57
HD 25123	G0	11	...	4.01	67	93	-30	-9	0.32	0.03	5.38	10.43
HD 40040	G0	12.4	11	4.12	65	44	-70	-12	0.31	0.07	4.45	8.53
HD 49409	G0V	11.2	8.2	4.30	53	110	-35	-62	0.37	1.53	5.10	11.07
HD 52711	G4V	7.9	5.1	4.53	19	-18	-78	-9	0.30	0.03	4.30	8.03
HD 60779	G0	6.8	5.3	4.38	36	-126	-57	-14	0.40	0.11	4.40	10.23
HD 67088	G5	13.7	...	4.63	67	95	-20	-7	0.31	0.05	5.67	10.86
HD 67587	F8	4.7	3.9	3.29	47	74	-56	0	0.32	0.12	4.77	9.28
HD 76095	G5V	5.5	5.3	3.28	49	2	-108	8	0.44	0.25	3.12	8.05
HD 77408	F6IV	3.7	4.3	3.52	50	-120	-10	-27	0.32	0.40	5.86	11.42
HD 78558	G0	11.6	10.9	4.44	37	-69	-74	-65	0.32	1.24	4.43	8.59
HD 88371	G2V	13.2	9.4	4.55	59	-135	-22	9	0.37	0.31	5.34	11.56
HD 88446	F8	7.3	7.8	3.77	67	-42	-98	4	0.41	0.17	3.45	8.16
HD 90508	G1V	10.4	7.4	4.63	23	21	-92	22	0.37	0.51	3.72	8.14
HD 109498	G3V	10.4	...	4.53	69	59	-46	-46	0.26	0.79	5.32	9.03
HD 111367	G1V	9.5	8.5	4.11	86	-69	-73	-45	0.33	0.76	4.34	8.53
HD 135694	K0	12.8	6.7	4.82	71	-36	-98	-39	0.40	0.57	3.50	8.10
HD 138750	F8	3.3	3.2	2.60	116	-72	-105	-16	0.46	0.18	3.07	8.37
HD 140209	G0	10.4	9.6	4.03	71	-73	-63	-29	0.30	0.37	4.62	8.62
HD 149105	G0V	6	5.8	3.37	53	49	-71	-10	0.32	0.06	4.35	8.53
HD 149890	F8V	6.8	6.1	4.15	39	60	-61	-29	0.31	0.38	4.69	8.82
HD 156617	G5	9.3	9.1	3.92	66	-102	-39	0	0.30	0.11	5.18	9.68
HD 156893	G5	8.9	8.5	3.74	77	-97	-65	56	0.35	1.60	4.47	9.19
HD 157214	G0V	13.9	8.1	4.60	14	25	-81	-64	0.32	1.33	4.21	8.17
BD +40 3374	K1	...	6.4	6.43	49	-109	-49	-58	0.34	1.15	4.88	9.88
HD 171009	G5	11.7	6.7	4.24	66	-68	-66	29	0.30	0.68	4.59	8.53
HD 171242	G0	9.2	8.5	4.02	62	103	-37	-2	0.35	0.10	5.03	10.55
HD 178478	G5	15.8	...	4.90	47	-86	-70	-12	0.35	0.08	4.26	8.86
HD 188326	G8IV	...	8.7	3.83	56	-91	-56	48	0.31	1.24	4.87	9.24
HD 206373	G0V	5.5	5.6	3.19	104	-37	-95	0	0.39	0.11	3.56	8.08
HD 210483	G1V	9.3	6.6	4.03	51	-77	-80	-17	0.37	0.15	3.96	8.63
HD 211476	G2V	7.1	6.7	4.59	31	-115	-35	-46	0.33	0.87	5.23	10.39
HD 217511	F5	2	2.1	2.23	122	-84	-55	-4	0.30	0.08	4.84	9.01
HD 219175	F9V	3.5	2.9	4.61	39	-92	-55	-14	0.31	0.10	4.79	9.19
					Thin-disc stars							
HD 115383	G0V	4.3	5.1	3.97	18	-38	2	-18	0.09	0.18	7.54	8.99
HD 127334	G5V	10.5	10.7	4.51	24	30	-4	-2	0.12	0.08	7.14	9.10
HD 136064	F9IV	3	3.7	3.12	25	62	-29	-24	0.23	0.29	5.83	9.37
HD 163989	F6IV	2.2	2.5	2.51	32	-29	-27	-22	0.10	0.22	6.64	8.16
HD 187013	F7V	2.8	...	3.34	22	38	-8	-25	0.14	0.28	6.88	9.20
HD 187691	F8V	3.3	3.1	3.71	19	-3	-3	-25	0.03	0.27	7.88	8.28
HD 200790	F8V	2.2	2.6	2.51	49	19	-37	10	0.15	0.27	6.03	8.21
HD 220117	F5V	1.8	1.6	2.66	42	-15	-21	-16	0.07	0.12	7.03	8.02
					Thick-disc stars							
HD 150433	G0	13.8	7.1	4.86	30	-8	-58	-46	0.21	0.73	5.21	7.97
HD 181047	G8V	13.9	10.2	4.96	47	-99	-43	-17	0.30	0.15	5.12	9.57
HD 186411	G0	6	...	3.36	88	-64	-56	-6	0.26	0.02	4.96	8.52
HD 195019	G3IV-V	9.7	8.6	3.96	39	-73	-76	-39	0.34	0.61	4.18	8.57
HD 198300	G0	10.3	7.1	4.89	53	81	-20	-24	0.28	0.28	5.84	10.26

Notes. [*] H09 - ages taken from Holmberg et al. (2009), C11 - from Casagrande et al. (2011).

random errors of atomic data and continuum placement and uncertainties in the stellar parameters. The sensitivity of the abundance estimates to changes in the atmospheric parameters by the assumed errors Δ[El/H][1] are illustrated for the star HD 52711 (Table 2). Clearly, possible parameter errors do not affect the abundances seriously; the element-to-iron ratios, which we use in our discussion, are even less sensitive.

The scatter of the deduced abundances from different spectral lines σ gives an estimate of the uncertainty due to the random errors. The mean value of σ is 0.04 dex, thus the uncertainties in the derived abundances that are the result of random errors amount to approximately this value.

---

[1] We use the customary spectroscopic notation $[X/Y] \equiv \log_{10}(N_X/N_Y)_{star} - \log_{10}(N_X/N_Y)_\odot$.
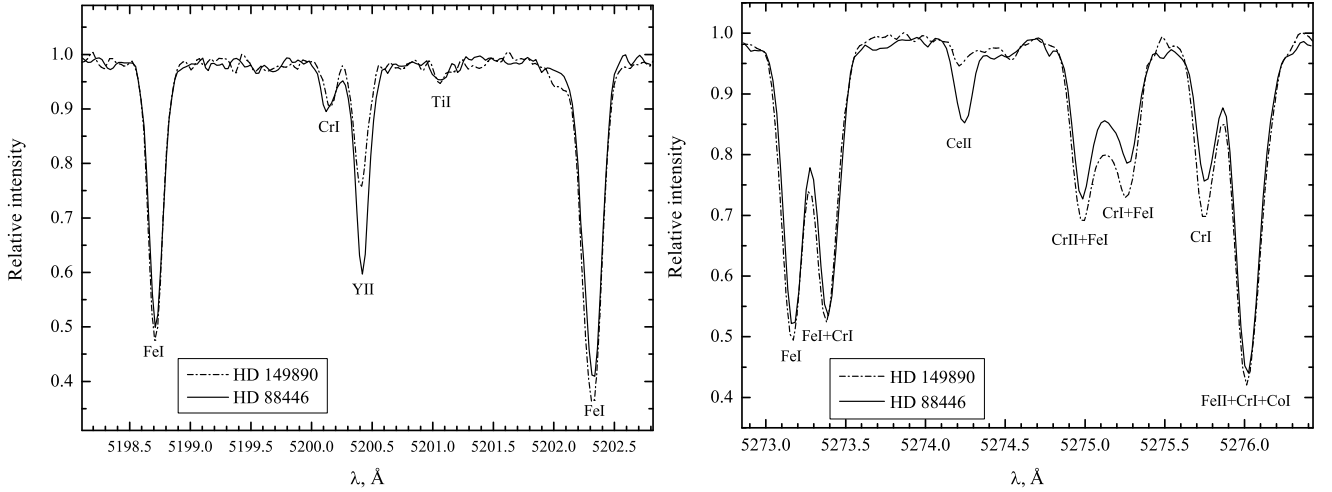
Fig. 6. NOT-FIES spectra of Group 1 stars HD 149890 and HD 88446. These two spectra are over-plotted to see the difference in spectral lines of elements produced in *s*-process, while lines of other chemical elements are similar.
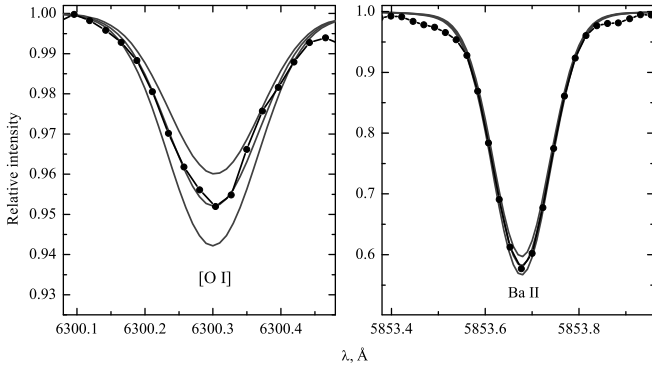

Fig. 3. Synthetic spectrum fit to the forbidden [O I] line at 6300.3 Å in the observed spectrum of HD 157214 (left panel) and to the barium line at 5853 Å in the observed spectrum of HD 52711. The observed spectra are shown by solid lines with dots. The dark grey solid lines are synthetic spectra with [O/Fe] = 0.42 ± 0.1 and with [Ba/Fe] = −0.08 ± 0.1, respectively.
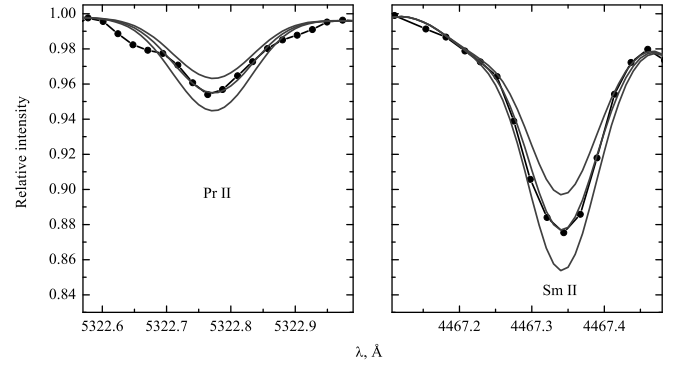
Fig. 4. Synthetic spectrum fit to the praseodymium line at 5323 Å in the observed spectrum of HD 3795 (left panel) and to the samarium line at 4467 Å in the observed spectrum of HD 22872. The observed spectra are shown by solid lines with dots. The dark grey solid lines are synthetic spectra with [Pr/Fe] = 0.54 ± 0.1 and [Sm/Fe] = 0.01 ± 0.1, respectively.

Effective temperatures for all stars investigated here are also available in Holmberg et al. (2009) and Casagrande et al. (2011). Casagrande et al. (2011) provided astrophysical parameters for the Geneva-Copenhagen survey by applying the infrared flux method to determine the effective temperature. In comparison to Holmberg et al. (2009), stars in the catalogue of Casagrande et al. (2011) are on average 100 K hotter. For the stars investigated here, our spectroscopic temperatures are on average only 40 ± 70 K hotter than in Holmberg et al. (2009) and 40 ± 90 K cooler than in Casagrande et al. (2011). The [Fe/H] values for all of the stars we investigated are available in Holmberg et al. (2009) as well as in Casagrande et al. (2011). A comparison between Holmberg et al. (2009) and Casagrande et al. (2011) shows that the latter gives [Fe/H] values that are more metal-rich on average by 0.1 dex. For our programme stars, we obtain a difference of 0.1 ± 0.1 dex in comparison with Holmberg et al. (2009) and we obtain no systematic difference, but a scatter of 0.1 dex, in comparison with Casagrande et al. (2011). The same result was found in comparing the atmospheric parameters determined for Group 3 stars in our Paper I and for Group 2 in Paper III.

Some stars from our sample were previously investigated by other authors. In Table 3, we present a comparison with results by Bensby et al. (2014) and Reddy et al. (2006), who investigated several stars in common with our work. Eight thin-disc stars that we investigated for a comparison have been analysed previously by Edvardsson et al. (1993). Slight differences in the $\log g$ values lie within the errors of uncertainties and are caused mainly by differences in the applied determination methods. We see that titanium and zirconium abundances determined using both neutral and ionised lines agree well and confirm the $\log g$ values determined using iron lines. Overall, our [El/Fe] for the stars in common agree very well with those in other studies.

3. Results and discussion

The atmospheric parameters, $T_{\rm eff}$, $\log g$, v_t, [Fe/H] and the abundances of 21 chemical elements relative to iron [El/Fe] of the programme and comparison stars are presented in Tables 4 and 5. The number of lines and the line-to-line scatter (σ) are presented as well.

The results are graphically displayed in Figs. 7 and 8. We display elemental abundance ratios of Group 1 stars together
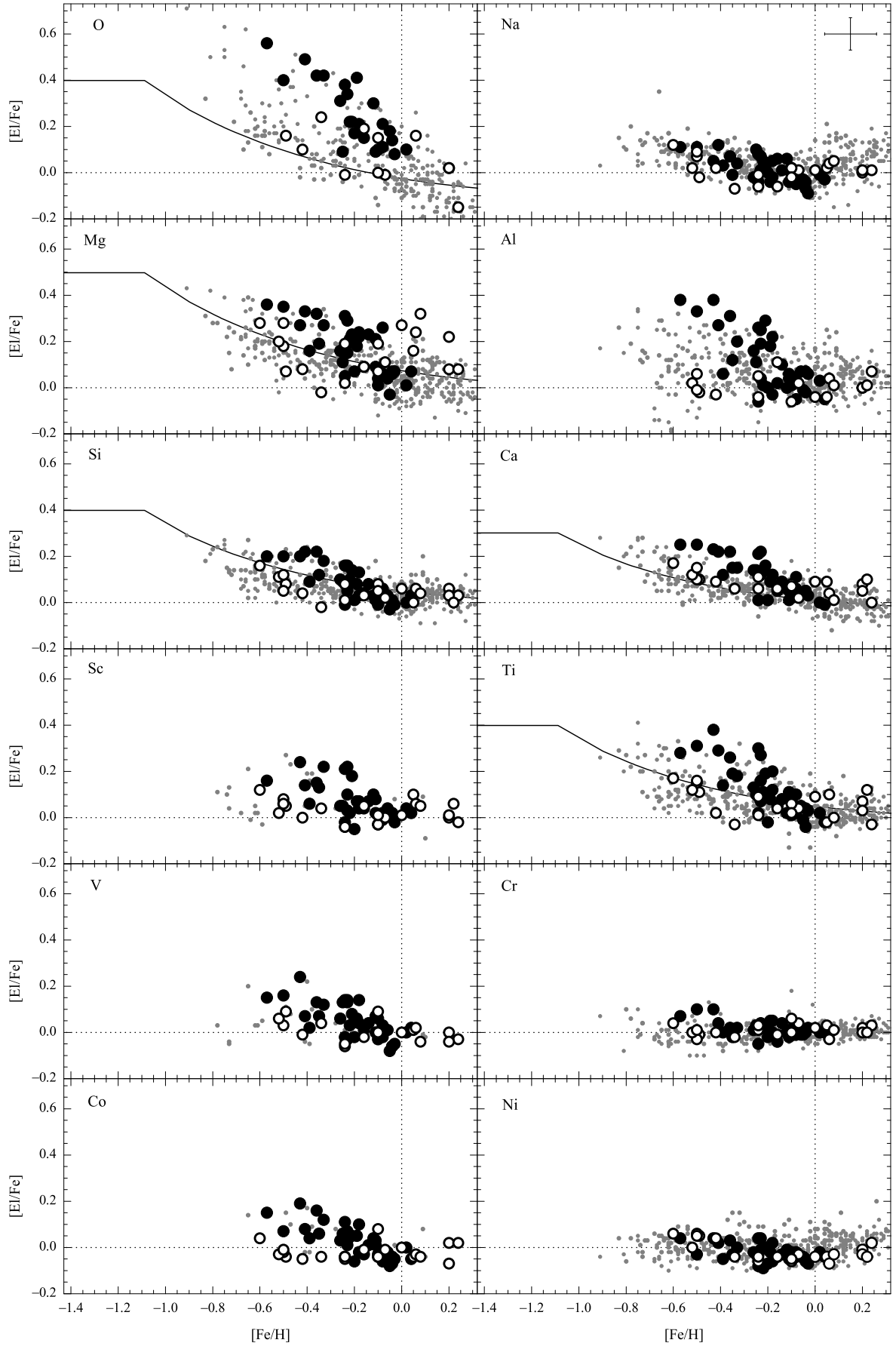
Fig. 7. [El/Fe] ratio as a function of [Fe/H] for Group 1 stars (filled circles) investigated here and for comparison thin-disc stars analysed in this work, Paper I, and Paper III (open circles). The data for the Milky Way thin-disc dwarfs taken from other studies are shown as a grey dots. Solid lines are Galactic thin-disc chemical evolution models presented by Pagel & Tautvaišienė (1995). Average uncertainties are shown in the box for Na.
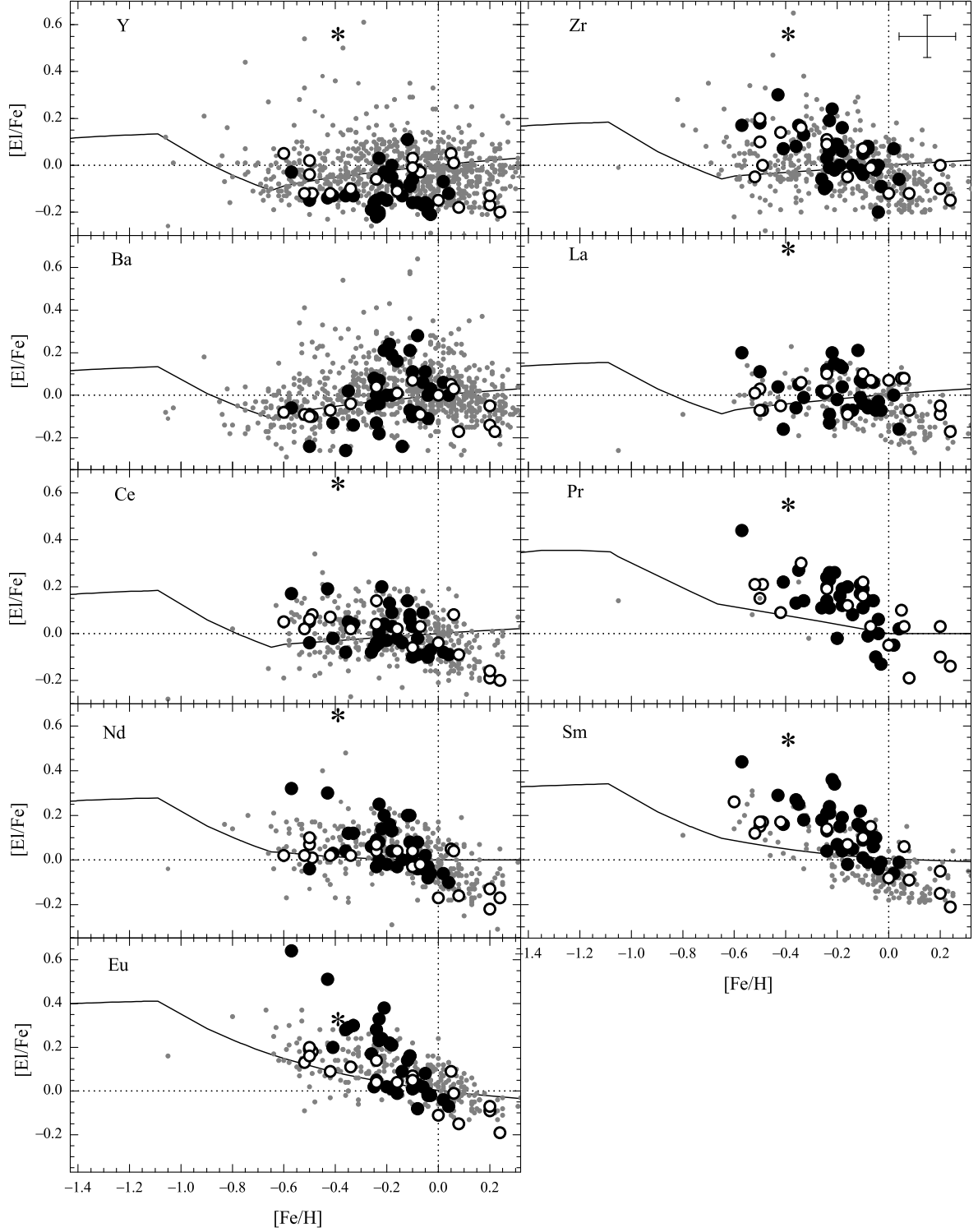
Fig. 8. [El/Fe] ratio as a function of [Fe/H] for Group 1 stars (filled circles) investigated here and for comparison thin-disc stars analysed in this work, Paper II, and Paper III (open circles). The s-process enhanced star (HD 88446) is marked as an asterisk. Grey dots correspond to the data for the Milky Way thin-disc dwarfs taken from other studies. The Galactic thin-disc chemical evolution model is shown as a solid line (Pagel & Tautvaišienė 1997). Average uncertainties are shown in the box for Zr.

with data of thin-disc stars investigated here and in Papers I, II, and III, as well as with results taken from other thin-disc studies (Edvardsson et al. 1993; Gratton & Sneden 1994; Koch & Edvardsson 2002; Bensby et al. 2005; Reddy et al. 2006; Zhang & Zhao 2006; Brewer & Carney 2006; Mashonkina et al. 2007, and Mishenina et al. 2013).

The chemical evolution models of the thin-disc were taken from Pagel & Tautvaišienė (1995, 1997). The thin-disc stars from Edvardsson et al. (1993) and Zhang & Zhao (2006) were selected using the membership probability evaluation method described by Trevisan et al. (2011), since their lists contained stars of other Galactic components as well. The same kine-

Fig. 5. Synthetic spectrum fit to the europium lines at 4129 Å and 6645 Å. The observed spectrum for the programme star HD 149105 is shown as a solid line with dots. The dark grey solid lines are synthetic spectra with [Eu/Fe] = 0.04 ± 0.1 and [Eu/Fe] = 0.11 ± 0.1 for these two lines, respectively.

Table 2. Effects on derived abundances resulting from model changes for the star HD 52711.

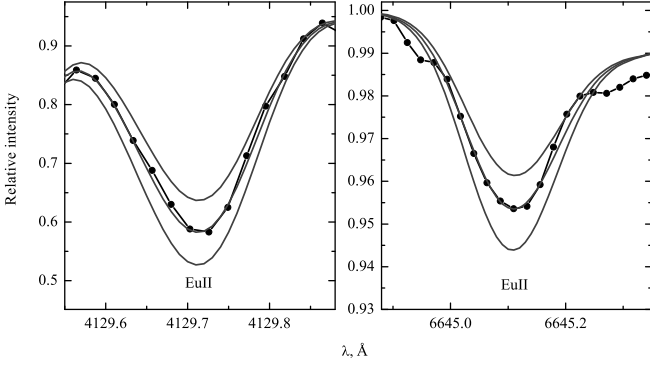| Ion	$\Delta T_{\rm eff}$ +100 K	$\Delta \log g$ +0.3	$\Delta v_{\rm t}$ +0.3 km s^{-1}	Total
[O I]	0.03	0.13	0.01	0.13
Na I	0.05	−0.02	−0.01	0.05
Mg I	0.05	−0.02	−0.03	0.06
Al I	0.04	0.00	0.00	0.04
Si I	0.03	0.01	−0.01	0.03
Ca I	0.07	−0.01	−0.02	0.07
Sc II	−0.00	0.11	−0.04	0.12
Ti I	0.09	0.00	−0.01	0.09
Ti II	0.01	0.12	−0.05	0.13
V I	0.11	−0.00	−0.01	0.11
Cr I	0.08	−0.02	−0.06	0.10
Cr II	−0.03	0.10	−0.09	0.14
Fe I	0.07	−0.02	−0.07	0.10
Fe II	−0.02	0.11	−0.07	0.13
Co I	0.08	0.01	−0.01	0.08
Ni I	0.06	−0.00	−0.04	0.07
Y II	0.02	0.10	−0.12	0.16
Zr I	0.11	0.01	0.01	0.11
Zr II	0.02	0.13	0.01	0.13
Ba II	0.06	0.08	−0.18	0.21
La II	0.03	0.12	0.01	0.12
Ce II	0.03	0.11	0.01	0.11
Pr II	0.02	0.12	0.01	0.12
Nd II	0.03	0.12	−0.01	0.12
Sm II	0.04	0.11	−0.01	0.12
Eu II	0.03	0.12	0.01	0.12

Notes. The table entries show the effects on the logarithmic abundances relative to hydrogen, Δ[El/H].

matic approach in assigning thin-disc membership was used in Bensby et al. (2005) and Reddy et al. (2006), which means that the thin-disc stars used for comparison are uniform in that respect.

One star in Group 1 is rich in elements predominantly produced in s-process. As shown in Table 5 and Figs. 6 and 8, HD 88446 has much stronger lines of elements predominantly produced in s-process and consequently much higher abundances of these elements. According to the definition of Beers & Christlieb (2005), HD 88446, with its [Ba/Fe] = 1.04

Table 3. Comparison with previous studies.

Quantity	Ours–B14	Ours–R06	Ours–E93
$T_{\rm eff}$	−31 ± 48	74 ± 51	−12 ± 65
log g	−0.18 ± 0.10	−0.16 ± 0.15	−0.28 ± 0.24
[Fe/H]	0.04 ± 0.05	0.09 ± 0.06	0.15 ± 0.06
[Na/Fe]	−0.01 ± 0.03	−0.05 ± 0.05	−0.05 ± 0.07
[Mg/Fe]	0.05 ± 0.08	−0.07 ± 0.05	0.06 ± 0.11
[Al/Fe]	0.00 ± 0.06	−0.02 ± 0.06	−0.11 ± 0.05
[Si/Fe]	0.01 ± 0.03	−0.03 ± 0.03	−0.02 ± 0.03
[Ca/Fe]	0.02 ± 0.03	0.04 ± 0.02	0.03 ± 0.05
[Sc/Fe]	...	0.01 ± 0.07	...
[Ti/Fe]	0.02 ± 0.04	0.06 ± 0.04	−0.04 ± 0.06
[V/Fe]	...	0.03 ± 0.05	...
[Cr/Fe]	0.01 ± 0.02	0.02 ± 0.03	...
[Co/Fe]	...	−0.01 ± 0.04	...
[Ni/Fe]	0.00 ± 0.03	−0.02 ± 0.02	−0.12 ± 0.05
[Y/Fe]	−0.05 ± 0.06	−0.10 ± 0.09	−0.12 ± 0.09
[Ba/Fe]	−0.02 ± 0.14	0.06 ± 0.13	−0.06 ± 0.18
[Ce/Fe]	...	0.01 ± 0.15	...
[Nd/Fe]	...	−0.06 ± 0.10	...
[Eu/Fe]	...	−0.02 ± 0.11	...

Notes. Mean differences and standard deviations of the main parameters and abundance ratios [El/Fe] for 13 stars of Group 1 in common with Bensby et al. (2014, B14), 7 stars of Group 1 in common with Reddy et al. (2006, R06), and 8 thin-disc stars in common with Edvardsson et al. (1993, E93).

and [Ba/Eu] = 0.70, falls in the category of the s-process-rich stars.

The metallicity of Group 1 stars we investigated lie in a broad interval of 0.04 ≥ [Fe/H] ≥ −0.57 with the average [Fe/H] equal to −0.20 ± 0.14 dex. Abundances of chemical elements are rather homogeneous and show similar overabundances of α-elements and r-process-dominated chemical elements with respect to thin-disc stars, as we also found for the stars of GCS Group 2 and 3. This elemental abundance pattern has similar characteristics with that in the Galactic thick-disc.

3.1. Comparison with the thick-disc

In Table 6 we present a comparison of mean [El/Fe] ratios calculated for stars of Group 1 and thick-disc stars at the same metallicity interval −0.57 < [Fe/H] < 0.04. Twenty-six thick-disc stars in this metallicity interval were investigated by Bensby et al. (2005), 37 stars by Reddy et al. (2006), 10 stars by Mashonkina et al. (2007), 51 stars by Stanford & Lambert (2012), and 7 stars by Mishenina et al. (2013). When comparing oxygen abundances, we did not use the results reported by Reddy et al. (2006) and Stanford & Lambert (2012) because they investigated the O I line, while we studied [O I]. The studies by Mashonkina et al. (2007) and Mishenina et al. (2013) were included in the comparison to enlarge the information on neutron capture elements. The average values of α-element abundances included Mg, Si, and Ca. Titanium was excluded because this element was not determined in one of the studies (Mishenina et al. 2013). The comparison shows that the deviations do not exceed the uncertainties.

Fig. 9 displays the comparison of [El/Fe] ratios for some chemical elements between individual stars in Groups 1, 2, and 3 and the thick-disc stars of the above-mentioned studies. For comparison, we selected oxygen, the averaged values for the α-elements Mg, Si, and Ca, and the s- and r-process-dominated elements barium and europium. Stars of the kinematic groups

Table 6. Comparison with thick-disc studies.

[El/Fe]	Ours–B14	Ours–R06	Ours–Ma07	Ours–S12	Ours–Mi13
[O/Fe]	−0.02	...	...	...	0.08
[Na/Fe]	−0.02	−0.06	...	−0.02	...
[Mg/Fe]	−0.03	−0.06	...	−0.01	−0.03
[Al/Fe]	−0.07	−0.12	...	−0.07	...
[Si/Fe]	−0.04	−0.10	...	−0.10	−0.06
[Ca/Fe]	0.01	−0.02	...	−0.02	−0.04
[Sc/Fe]	...	−0.06	...	−0.11	...
[Ti/Fe]	−0.05	−0.04	...	−0.01	...
[V/Fe]	...	−0.06	...	−0.04	...
[Cr/Fe]	0.01	0.03	...	−0.05	...
[Co/Fe]	...	−0.06	...	−0.05	...
[Ni/Fe]	−0.03	−0.05	...	−0.02	−0.05
[Y/Fe]	−0.09	−0.08	−0.13	−0.11	−0.11
[Zr/Fe]	...	...	−0.07	...	0.02
[Ba/Fe]	0.05	0.12	0.11	0.07	0.06
[La/Fe]	...	...	...	...	0.10
[Ce/Fe]	...	−0.07	−0.06	−0.08	0.02
[Nd/Fe]	...	−0.09	...	−0.06	−0.05
[Sm/Fe]	...	...	...	...	0.02
[Eu/Fe]	...	−0.14	...	−0.17	−0.06

Notes. Differences of mean [El/Fe] values for stars of Group 1 and thick-disc stars at the same metallicity interval −0.57 < [Fe/H] < 0.04. Sixty-three stars from Bensby et al. (2014, B14), 37 stars from Reddy et al. (2006, R06), 10 stars from Mashonkina et al. (2007, Ma07), 51 stars from Stanford & Lambert (2012, S12), and 10 stars from Mishenina et al. (2013, Mi13).

and of the thick disc have very similar chemical compositions. We have observed and analysed several thick-disc stars as well. Their elemental abundance ratios are also plotted in Fig. 9 and agree well with results of the programme stars. Thus, the chemical composition of all three GCS kinematic groups is similar to the thick-disc stars, which might suggest that their formation histories are linked.

3.2. Age

According to Helmi et al. (2006), the stars in Group 1 fall into two age populations: 33% of the stars are 8 Gyr old, and 67% are 12 Gyr old. The ages were later redetermined by Holmberg et al. (2009) and Casagrande et al. (2011) and agree with each other within uncertainties (we present them in Table 1). Holmberg et al. (2009) present upper and lower age limits for every star. The average lower and upper limit is 10 and 14 Gyr for stars of the 12 Gyr age population, 7 and 10 Gyr for the 8 Gyr population, and 4 and 5 Gyr for the younger stars, respectively. Fig. 10 shows the Group 1 stars investigated here with our spectroscopic effective temperatures and absolute magnitudes M_v, taken from Holmberg et al. (2009), in a Hertzsprung-Russell (HR) diagram. The isochrones were taken from Bressan et al. (2012). The overall features of stars in the diagrams are well reproduced by isochrones of the two indicated ages. The more metal-abundant stars fit the 8 Gyr isochrone quite well, while more metal-deficient stars fit the 12 Gyr isochrone (for metal-deficient stars, the isochrones are with [α/Fe]= 0.2). A subgroup of ten stars in our sample are younger (2 Gyr $\leq$ age $\leq$ 5 Gyr) and in the HR diagram lie higher than the turnoff luminosity of the 8 Gyr isochrone. The number of stars younger than 5 Gyr among 120 stars in Group 1 is 18 (according to ages determined by Holmberg et al. 2009). A subgroup of about 15
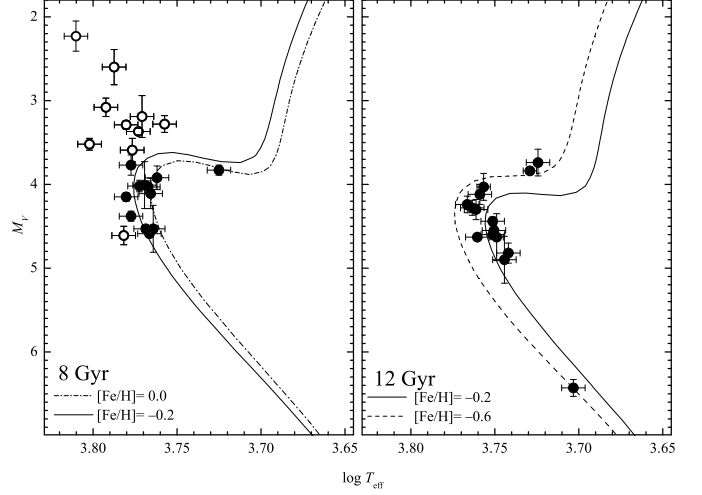
Fig. 10. HR diagrams of the Group 1 stars. Isochrones are taken from Bressan et al. (2012). The isochrones for metal-deficient stars are with [α/Fe]= 0.2. The open circles represent the younger stars with ages of 2–5 Gyr.

young main-sequence stars can be separated among 86 Group 2 stars as well (Paper III). The chemical composition pattern of the young stars we investigated is similar to the rest of the GCS kinematic group stars of the same metallicity.

3.3. Comparison with kinematic streams

In this subsection, we discuss the GCS kinematic groups in the context of three other Galactic kinematic substructures of similar metallicities. Our attention was attracted by the Hercules stream. Stars of this kinematic stream have a similar range of metallicities and ages to those in the GCS groups (Bobylev & Bajkova 2007; Antoja et al. 2008; Bensby et al. 2007, 2014). The Hercules stream was first identified by Eggen (1958) as a group of 22 stars with velocities similar to the high velocity star ξ Herculis (HD 150680). It is believed that the Hercules stream is a result of resonant interactions between stars in the outer disc and the Galactic bar. This stellar stream is a heterogeneous group of objects from the thin and thick discs (Dehnen 2000; Fux 2001; Quillen 2003; Famaey et al. 2005; Soubiran & Girard 2005; Pakhomov et al. 2011; Antoja et al. 2014; Bensby et al. 2014).

The origin of the Arcturus stream has been debated for years (Eggen 1971, 1996, 1998; Arifyanto & Fuchs 2006; Gilmore et al. 2002; Wyse et al. 2006; Bensby et al. 2014, and references therein). Stars of the Arcturus stream were identified by Gilmore et al. (2002), and later Wyse et al. (2006), as a group of stars lagging behind the local standard of rest (LSR) by about 100 km s^{-1}. This stream was associated with a disrupted satellite that merged with the Milky Way 10–12 Gyr ago. Navarro et al. (2004) suggested that these stars are the same group of stars that Eggen (1971) associated with the bright star Arcturus, whose Galactic orbital velocity also lags at the same value. Navarro et al. (2004) analysed the group of stars associated kinematically with Arcturus and confirmed that they constitute a peculiar grouping of metal-poor stars with a similar apocentric radius, a common angular momentum, and distinct metal abundance patterns. These properties are consistent with those expected for a group of stars originating from the debris of a disrupted satellite. Navarro et al. (2004) also noticed that the angu-
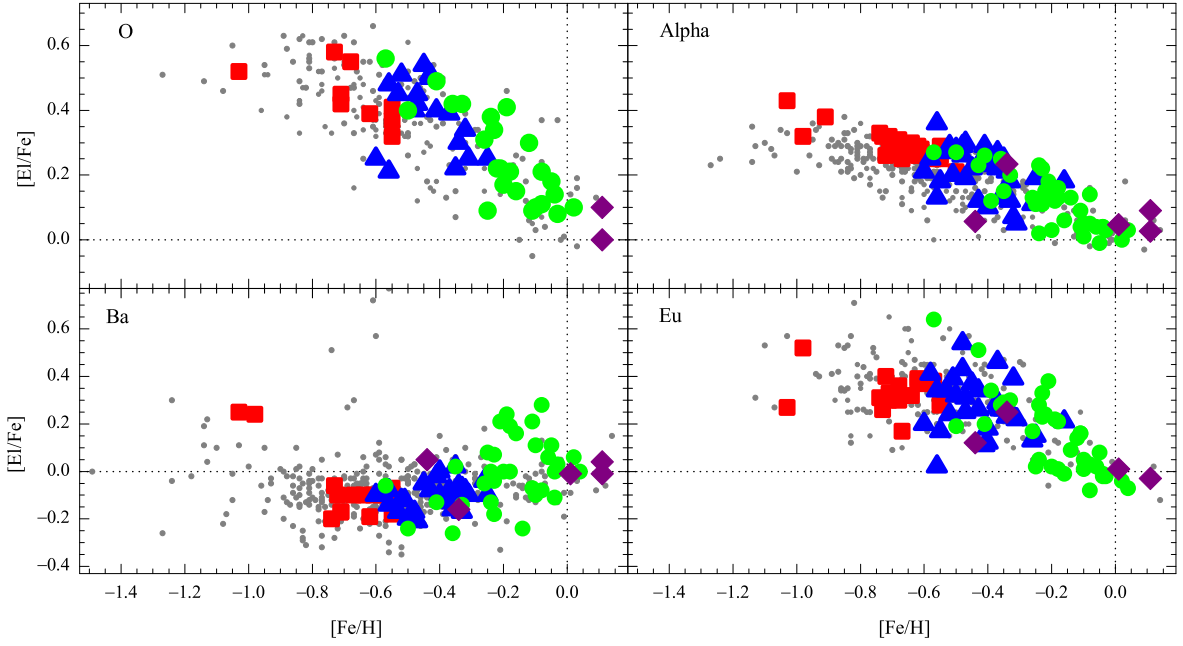
Fig. 9. [El/Fe] ratio as a function of [Fe/H] in the Group 1 stars (green dots) investigated here, Group 2 (blue triangles, Paper III), Group 3 (red squares, Papers I and II), and comparison thick-disc stars (purple diamonds). The literature data for the Milky Way thick-disc stars are shown as a grey dots. The averaged values for α-elements consist of Mg, Si, and Ca abundances.

lar momentum of such a group is too low to arise from dynamical perturbations induced by the Galactic bar. More recently, Gardner & Flynn (2010) and Monari et al. (2013) showed that the Galactic long bar may produce a kinematic feature in velocity space with the same parameters as occupied by the Arcturus moving group.

Another so-called AF06 stellar stream was discovered by Arifyanto & Fuchs (2006) while analysing the fine structure of the phase space distribution function of nearby subdwarfs using data extracted from various catalogues. According to the discoverers, AF06 possibly resembles the Arcturus stream.

Fig. 11 presents a Toomre diagram and velocity distributions of stars in the GCS kinematic groups and Hercules, Arcturus, and AF06 streams. This diagram shows that the kinematics of stars in the GCS groups is quite different from the displayed streams, and only AF06 partially overlaps the pattern.

A comparison of [El/Fe] ratios for α-elements between individual stars in the GCS groups and stars of the Arcturus, AF06, and Hercules streams is presented in Fig.12. The averaged values for α-elements consist of Mg, Si, Ca, and Ti abundances. We took the elemental abundances for 33 stars of the Hercules stream from Soubiran & Girard (2005) and for 35 stars from Bensby et al. (2014). We took the elemental abundances for 18 stars of the Arcturus stream and for 26 stars of the AF06 stream from Ramya et al. (2012). In Fig.12 we also show the chemical evolution model of the Galactic thin-disc by Pagel & Tautvaišienė (1995) and a simple second-order polynomial fit to the GCS kinematic group stars.

The element-to-iron ratios in the GCS kinematic stellar groups lie higher than in the majority of stars belonging to Arcturus, AF06, and Hercules streams. The AF06 group has the chemical composition most similar to the GCS stars. In Paper III, we pointed out that the Arcturus group has thick-disc kinematics, but it has seemingly thin-disc abundances. Finally, as noted previously, the stars associated with the Hercules stream do not have a distinct chemical signature, but show a mixture of abun-

dances as seen in the thin and thick discs (c.f. Soubiran & Girard 2005; Bensby et al. 2007, 2014; Pakhomov et al. 2011).

Thus, the presented comparison of kinematic and chemical composition patterns in the Galactic substructures, leads us to the conclusion that the origin of the GCS kinematic stellar groups was different from Galactic streams that originated in a course of the resonant interactions between stars in the outer disc and the Galactic bar.

3.4. Origin

A sample of 274 stars was identified as an overdensity in the eccentricity range $0.3 < \epsilon < 0.5$ in the Geneva-Copenhagen survey by Helmi et al. (2006). The authors provide statistical evidence that these overdensities are real, and that they do not result from a poor choice of the comparison model of the Galaxy or uncertainties of eccentricity determinations. It was found that stars with these dynamical characteristics do not constitute a homogeneous population. The metallicity distribution of the stars in this overdense region of the APL-space varied with eccentricity in a discontinuous fashion. This allowed the authors to separate these stars into three kinematic groups. These three groups of stars are dissimilar not only in their metallicity distribution, but they also have different kinematics in the vertical (z) direction. The Group 1 velocity dispersion has σ_z about 28 km s^{-1}, that of Group 2 about 39 km s^{-1}, and that of Group 3 about 52 km s^{-1}.

Helmi et al. (2014) determined the detailed chemical composition for 36 stars of the GCS Group 1, for 22 stars of Group 2, and 14 stars of Group 3 located in the southern hemisphere. In this study, they noticed a relatively sharp transition in dynamical and chemical properties that occurs at a metallicity of [Fe/H] ~ -0.4. In their sample, stars with [Fe/H] > -0.4 have mostly lower eccentricities, smaller vertical velocity dispersions, are α-enhanced, and define a rather narrow sequence in [α/Fe] versus [Fe/H], clearly distinct from that of the thin disc. Stars with [Fe/H] < -0.4 have a range of eccentricities, are hotter

10
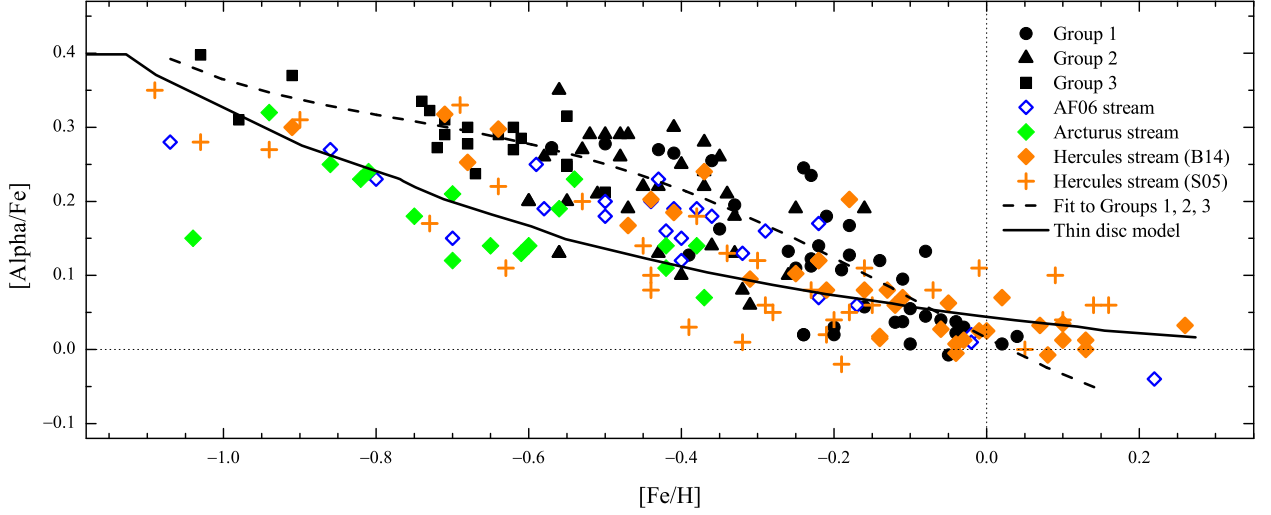
Fig. 12. [α/Fe] ratio as a function of [Fe/H] in the GCS kinematic group of stars, in the Arcturus stream (green diamonds), in the AF06 stream (blue empty diamonds), and in the Hercules stream (orange diamonds and crosses). The data for Arcturus and AF06 streams were taken from Ramya et al. (2012), for the Hercules stream from Soubiran & Girard (2005) and Bensby et al. (2014). The averaged values for α-elements consist of Mg, Si, Ca, and Ti abundances. A thin-disc model (continuous line) is taken from Pagel & Tautvaišienė (1995), the 2nd order polynomial fit to the GCS data is shown by the dashed line.
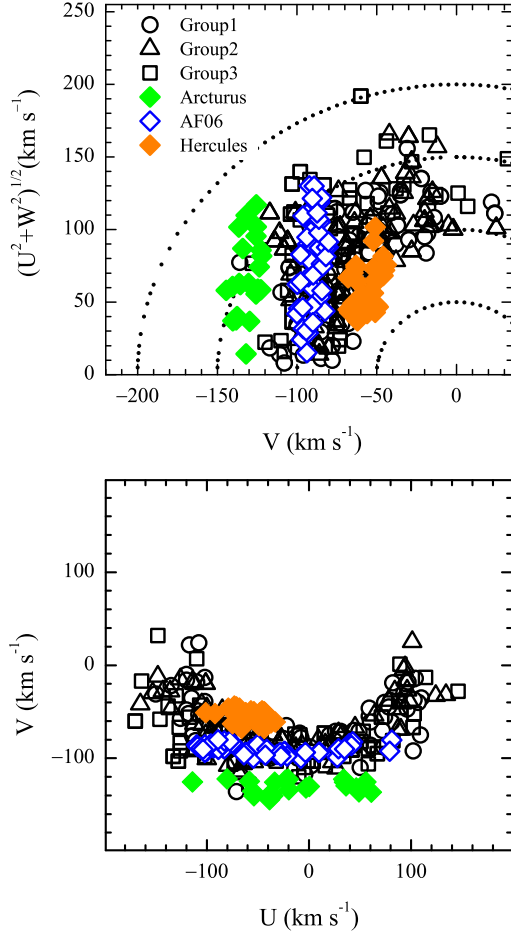
Fig. 11. Upper panel: Toomre diagram of stars in GCS kinematic groups and Arcturus, AF06, and Hercules streams. Dotted lines indicate constant values of total space velocity in steps of 50 km s^{-1}. Lower panel: Velocity distribution for stars in the same kinematic groups and streams.

vertically, and depict a larger spread in [α/Fe]. Looking at our slightly larger sample of GCS kinematic group stars (Fig. 13) investigated here, we agree with Helmi et al. (2014) that stars with lower metallicities have a wider range of eccentricities than those that are more metal-abundant. However, the spread of [α/Fe], seems to be about the same at all metallicities (see Fig. 9 and Fig. 12). In Fig. 13, we mark stars of different ages with different colours. Practically all stars with [Fe/H] > −0.4 have ages around 12 Gyr, while the youngest stars are predominantly metal-abundant.

Even though, according to the dynamical characteristics, the stars of the GCS kinematic groups do not constitute a homogeneous population, their similar chemical composition pattern indicates that these kinematic groups might share a similar origin. The similarity in chemical composition of stars in these kinematic groups and in the thick-disc of the Galaxy suggests that the formation histories of these groups and the thick-disc might be linked. This circumstance led us to look for the currently available thick-disc formation scenario, which allows for the presence of stars with GCS kinematic group characteristics. As we pointed out in Papers I, II, and III, the kinematic properties of the GCS kinematic groups fit a gas-rich satellite merger scenario (Brook et al. 2004, 2005; Dierickx et al. 2010; Wilson et al. 2011; Di Matteo et al. 2011) best of all. Within this particular scenario, the eccentricities of accreted stars peak at about 0.3 < ϵ < 0.5 (Sales et al. 2009), which are exactly the characteristics of the GCS groups that we investigated. The gas-rich merger scenario is worth considering since, according to Dierickx et al. (2010), it fits the thick-disc star eccentricity distribution better than the accretion, heating, or migration scenarios. Although it is likely that all of those processes to some extent acted in the Milky Way, it is not clear which, if any, was the dominant mechanism.

Finally, the numerical simulations of the disruption of a satellite galaxy that falls into its parent galaxy shows that the satellite debris can end up in several cold star streams with roughly the same characteristic eccentricities of their orbits (Helmi et al. 2006). The possibility of such a scheme and the similar properties of element-to-iron ratios found in the GCS
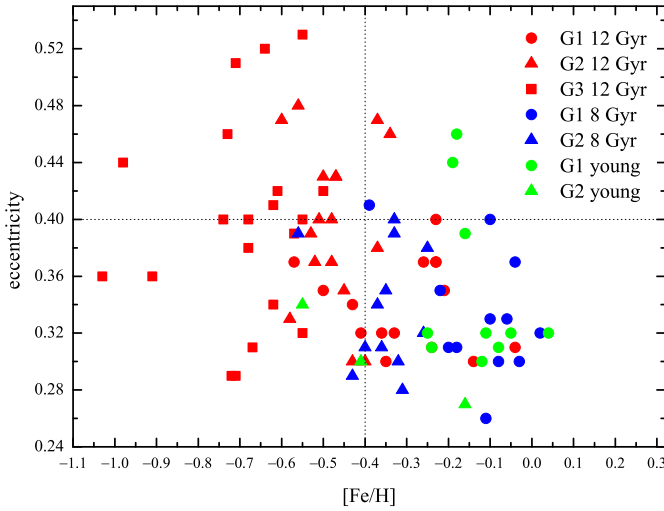
Fig. 13. Eccentricity and [Fe/H] diagram of the GCS kinematic group stars. The red symbols correspond to stars investigated here with ages of about 12 Gyr, blue to about 8 Gyr, and green to the younger stars in Groups 1, 2, and 3.

kinematic groups lead to the assumption that the GCS kinematic star groups might belong to the same satellite galaxy and might have originated in our Galaxy during the same merging event.

Investigations of formation and evolution of the Milky Way discs are continuing both observationally (e.g. Haywood et al. 2013; Kordopatis et al. 2013b; Anders et al. 2014; Bensby et al. 2014; Bergemann et al. 2014; Mikolaitis et al. 2014) and theoretically (Micali et al. 2013; Snaith et al. 2014; Robin et al. 2014; Kubryk et al. 2014; Minchev et al. 2014, and references therein). A model that could reproduce well the present day values of all of the main global observables of the Milky Way disc has not been discovered yet.

4. Conclusions

We measured abundances of 22 chemical elements from high-resolution spectra in 37 stars belonging to Group 1 of the Geneva-Copenhagen survey. This kinematically identified group of stars as well as two other GCS kinematic groups was suggested to be a remnant of a disrupted satellite galaxy. Our main goal was to investigate the chemical composition of stars within Group 1, to compare it with the relative abundance patterns in the Galactic thin- and thick-disc stars, in the GCS Group 2 and Group 3 stars, as well as in several kinematic streams of similar metallicities.

Our study shows the following:

1. The metallicities of the investigated stars in Group 1 are in the range of $0.04 \geq [Fe/H] \geq -0.57$. The average [Fe/H] value is -0.20 ± 0.14 dex.
2. Investigated Group 1 stars can be separated into three age subgroups. Along with the main 8- and 12-Gyr-old populations, a subgroup of stars younger than 5 Gyr can be separated as well.
3. All programme stars have higher abundances in oxygen, α-elements, and r-process-dominated chemical elements than Galactic thin-disc dwarfs and the Galactic evolution model. The abundances of iron-group chemical elements and elements produced mainly by the s-process are similar to those in the Galactic thin-disc dwarfs of the same metallicity.

4. The chemical composition and kinematic properties in the GCS Group 1, 2, and 3 stars are different from those in stars of the Hercules, Arcturus and AF06 streams.
5. The chemical composition patterns in GCS Groups 1, 2, and 3 are similar to each other and to the thick-disc stars, which might suggest that their formation histories are linked.
6. The chemical composition together with the kinematic properties and ages of stars in the investigated GCS Group 1, 2 and 3 support a gas-rich satellite merger scenario as a possible origin for these kinematic groups.

References

Anders, F., Chiappini, C., Santiago, B. X., et al. 2014, A&A, 564, AA115
Antoja, T., Figueras, F., Fernández, D., & Torra, J. 2008, A&A, 490, 135
Antoja, T., Helmi, A., Bienayme, O., et al. 2012, MNRAS, 426, 1
Antoja, T., Helmi, A., Dehnen, W., et al. 2014, A&A, 563, 60
Arifyanto, M. I., & Fuchs, B. 2006, A&A, 449, 533
Beers, T. C., & Christlieb, N. 2005, ARA&A, 43, 531
Bensby, T., Oey, M. S., Feltzing, S., & Gustafsson, B. 2007, ApJ, 655, L89
Bensby, T., Feltzing, S., & Oey, M. S. 2014, A&A, 562, A71
Bensby, T., Feltzing, S., Lundström, I., & Ilyin, I. 2005, A&A, 433, 185
Bergemann, M., Ruchti, G. R., Serenelli, A., et al. 2014, A&A, 565, AA89
Bobylev, V. V., & Bajkova, A. T. 2007, Astronomy Reports, 51, 372
Bobylev, V. V., Bajkova, A. T., & Mylläri, A. A. 2010, Astronomy Letters, 36, 27
Bressan, A., Marigo, P., Girardi, L., Salasnich, B., Dal Cero, C., Rubele, S., Nanni, A. 2012, MNRAS, 427, 127
Brewer, M.-M., & Carney, B. W. 2006, AJ, 131, 431
Brook, C. B., Gibson, B. K., Martel, H., & Kawata, D. 2005, ApJ, 630, 298
Brook, C. B., Kawata, D., Gibson, B. K., & Freeman, K. C. 2004, ApJ, 612, 894
Casagrande, L., Schönrich, R., Asplund, M., et al. 2011, A&A, 530, A138
Dehnen, W. 2000, AJ, 119, 800
Dekker, E. 1976, Phys. Rep., 24, 315
Dettbarn, C., Fuchs, B., Flynn, C., & Williams, M. 2007, A&A, 474, 857
Di Matteo, P., Lehnert, M. D., Qu, Y., & van Driel, W. 2011, A&A, 525, L3
Dierickx, M., Klement, R., Rix, H.-W., & Liu, C. 2010, ApJ, 725, L186
Edvardsson, B., Andersen, J., Gustafsson, B., et al. 1993, A&A, 275, 101
Eggen, O. J. 1958, MNRAS, 118, 154
Eggen, O. J. 1971, PASP, 83, 271
Eggen, O. J. 1996, AJ, 112, 1595
Eggen, O. J. 1998, AJ, 115, 2397
Famaey, B., Jorissen, A., Luri, X., et al. 2005, A&A, 430, 165
Flynn, C., Sommer-Larsen, J., & Christensen, P. R. 1996, MNRAS, 281, 1027
Fux, R. 2001, A&A, 373, 511
Gardner, E., & Flynn, C. 2010, MNRAS, 405, 545
Gilmore, G., & Reid, N. 1983, MNRAS, 202, 1025
Gilmore, G., Wyse, R. F. G., & Norris, J. E. 2002, ApJ, 574, L39
Gómez, F. A., Minchev, I., Villalobos, Á., O'Shea, B. W., & Williams, M. E. K. 2012, MNRAS, 419, 2163
Gratton, R. G., & Sneden, C. 1994, A&A, 287, 927
Grevesse, N., & Sauval, A. J. 2000, Origin of Elements in the Solar System, Implications of Post-1957 Observations, 261
Gurtovenko, E. A., & Kostyk, R. I. 1989, Kiev Izdatel Naukova Dumka,
Gustafsson, B., Edvardsson, B., Eriksson, K., et al. 2008, A&A, 486, 951
Haywood, M., Di Matteo, P., Lehnert, M. D., Katz, D., & Gómez, A. 2013, A&A, 560, AA109
Helmi, A. 2004, ApJ, 610, L97
Helmi, A., Navarro, J. F., Nordström, B., et al. 2006, MNRAS, 365, 1309
Helmi, A., Williams, M., Freeman, K. C., Bland-Hawthorn, J., & De Silva, G. 2014, ApJ, 791, 135
Holmberg, J., Nordström, B., & Andersen, J. 2009, A&A, 501, 941
Ilyin, I. V. 2000, Ph.D. dissertation, Univ. Oulu, Finland
Kirby, E. N., Lanfranchi, G. A., Simon, J. D., Cohen, J. G., & Guhathakurta, P. 2011, ApJ, 727, 78

Klement, R. 2010, A&A Rev., 18, 567

Klement, R., Fuchs, B., & Rix, H.-W. 2008, ApJ, 685, 261

Klement, R., Rix, H.-W., Flynn, C., et al. 2009, ApJ, 698, 865

Klement, R. J., Bailer-Jones, C. A. L., Fuchs, B., Rix, H.-W., & Smith, K. W. 2011, ApJ, 726, 103

Koch, A., & Edvardsson, B. 2002, A&A, 381, 500

Kordopatis, G., Hill, V., Irwin, M., et al. 2013a, A&A, 555, A12

Kordopatis, G., Gilmore, G., Wyse, R. F. G., et al. 2013b, MNRAS, 436, 3231

Kubryk, M., Prantzos, N., & Athanassoula, E. 2014, arXiv:1412.0585

Kurucz, R. L. 2005, Memorie della Societa Astronomica Italiana Supplementi, 8, 189

Law, D. R., Johnston, K. V., & Majewski, S. R. 2005, ApJ, 619, 807

Monari, G., Antoja, T., & Helmi, A. 2013, arXiv:1306.2632

Mashonkina, L. I., Vinogradova, A. B., Ptitsyn, D. A., Khokhlova, V. S., & Chernetsova, T. A. 2007, Astronomy Reports, 51, 903

Micali, A., Matteucci, F., & Romano, D. 2013, MNRAS, 436, 1648

Mikolaitis, Š., Hill, V., Recio-Blanco, A., et al. 2014, A&A, 572, AA33

Minchev, I., Chiappini, C., & Martig, M. 2014, A&A, 572, AA92

Minchev, I., Quillen, A. C., Williams, M., et al. 2009, MNRAS, 396, L56

Mishenina, T. V., Pignatari, M., Korotin, S. A., et al. 2013, A&A, 552, A128

Navarro, J. F., Helmi, A., & Freeman, K. C. 2004, ApJ, 601, L43

Nordström, B., Mayor, M., Andersen, J., et al. 2004, A&A, 418, 989

Pagel, B. E. J., & Tautvaišienė, G. 1997, MNRAS, 288, 108

Pagel, B. E. J., & Tautvaišienė, G. 1995, MNRAS, 276, 505

Pakhomov, Y. V., Antipova, L. I., & Boyarchuk, A. A. 2011, Astronomy Reports, 55, 256

Pauli, E.-M., Napiwotzki, R., Altmann, M., et al. 2003, A&A, 400, 877

Peñarrubia, J., Martínez-Delgado, D., Rix, H. W., et al. 2005, ApJ, 626, 128

Perryman, M. A. C., de Boer, K. S., Gilmore, G., et al. 2001, A&A, 369, 339

Piskunov, N. E., Kupka, F., Ryabchikova, T. A., Weiss, W. W., & Jeffery, C. S. 1995, A&AS, 112, 525

Quillen A. C. 2003, AJ, 125, 785

Ramya, P., Reddy, B. E., & Lambert, D. L. 2012, MNRAS, 425, 3188

Reddy, B. E., Lambert, D. L., & Allende Prieto, C. 2006, MNRAS, 367, 1329

Robin, A. C., Reylé, C., Fliri, J., et al. 2014, A&A, 569, AA13

Sales, L. V., Helmi, A., Abadi, M. G., et al. 2009, MNRAS, 400, L61

Snaith, O. N., Haywood, M., Di Matteo, P., et al. 2014, ApJ, 781, LL31

Stanford, L. M., & Lambert, D. L. 2012, MNRAS, 424, 2118

Stonkutė, E., Tautvaišienė, G., Nordström, B., & Ženovienė, R. 2012, A&A, 541, A157 (Paper I)

Stonkutė, E., Tautvaišienė, G., Nordström, B., & Ženovienė, R. 2013, A&A, 555, A6 (Paper II)

Soubiran, C., & Girard, P. 2005, A&A, 438, 139

Trevisan, M., Barbuy, B., Eriksson, K., et al. 2011, A&A, 535, A42

Villalobos, Á., & Helmi, A. 2009, MNRAS, 399, 166

Villalobos, Á., & Helmi, A. 2008, MNRAS, 391, 1806

Wilson, M. L., Helmi, A., Morrison, H. L., et al. 2011, MNRAS, 413, 2235

Wu, Z.-Y., Zhou, X., Ma, J., & Du, C.-H. 2009, MNRAS, 399, 2146

Wyse, R. F. G., Gilmore, G., Norris, J. E., et al. 2006, ApJ, 639, L13

Ženovienė, R., Tautvaišienė, G., Nordström, B., & Stonkutė, E. 2014, A&A, 563, A53 (Paper III)

Zhang, H. W., & Zhao, G. 2006, A&A, 449, 127

Table .4. Main atmospheric parameters and elemental abundances of programme and comparison stars.

Star	$T_{\rm eff}$ K	log g	v_t km s^{-1}	[Fe/H]	$\sigma_{\rm FeI}$	$n_{\rm FeI}$	$\sigma_{\rm FeII}$	$n_{\rm FeII}$	[O/Fe]	[Na/Fe]	σ	n	[Mg/Fe]	σ	n
Group 1 stars															
HD 3795	5360	3.7	1.0	-0.57	0.05	31	0.04	6	0.56	0.11	0.02	4	0.36	0.05	4
HD 4607	6200	3.8	1.2	-0.08	0.05	25	0.03	6	0.21	0.00	0.02	2	0.26	0.00	3
HD 15777	5800	4.2	1.0	-0.33	0.04	28	0.04	6	0.42	0.04	0.01	5	0.27	0.06	3
HD 22872	5980	4.0	1.1	0.04	0.05	34	0.02	8	...	-0.03	0.01	3	0.07	0.09	4
HD 25123	5880	3.9	1.1	0.02	0.04	37	0.06	8	0.10	-0.01	0.01	5	0.01	0.02	3
HD 40040	5740	4.0	1.1	-0.24	0.05	37	0.05	7	0.38	0.08	0.02	3	0.31	0.06	4
HD 49409	5770	4.1	0.9	-0.23	0.04	32	0.04	6	...	0.01	0.02	3	0.15	0.05	4
HD 52711	5870	4.1	1.0	-0.08	0.05	38	0.03	7	0.11	-0.05	0.01	4	0.06	0.05	4
HD 60779	5990	4.1	0.9	-0.10	0.05	36	0.04	8	0.10	0.02	0.03	4	0.04	0.03	3
HD 67088	5610	4.0	0.8	-0.04	0.04	37	0.03	7	0.14	-0.07	0.04	5	0.07	0.05	4
HD 67587	6030	3.8	1.1	-0.25	0.05	34	0.05	8	0.09	0.10	0.03	4	0.11	0.03	3
HD 76095	5720	4.1	1.0	-0.19	0.04	35	0.05	8	0.41	-0.04	0.01	4	0.18	0.05	4
HD 77408	6340	4.2	1.1	-0.11	0.04	25	0.04	7	...	-0.04	0.05	3	0.21	0.11	3
HD 78558	5640	4.0	0.9	-0.41	0.05	36	0.04	7	0.49	0.12	0.06	5	0.33	0.07	4
HD 88371	5630	4.2	0.8	-0.23	0.04	38	0.06	8	0.34	0.01	0.05	5	0.29	0.06	4
HD 88446	5990	3.9	1.2	-0.39	0.05	34	0.03	8	...	0.03	0.04	3	0.16	0.04	3
HD 90508	5760	4.1	1.0	-0.26	0.04	37	0.05	8	0.31	-0.02	0.06	5	0.16	0.01	4
HD 109498	5810	4.2	1.0	-0.11	0.06	30	0.06	6	0.09	0.01	0.06	4	0.09	0.02	3
HD 111367	5830	4.0	1.0	-0.06	0.05	34	0.05	8	...	-0.03	0.01	4	0.04	0.05	3
HD 135694	5520	3.9	0.9	-0.23	0.06	24	0.06	5	...	0.07	0.01	3	0.19	0.09	2
HD 138750	6130	3.8	1.1	-0.18	0.05	33	0.04	8	...	-0.02	0.00	3	0.24	0.05	3
HD 140209	5710	4.0	1.1	-0.14	0.05	28	0.03	5	...	0.01	0.05	5	0.23	0.08	4
HD 149105	5930	3.8	1.0	-0.05	0.04	30	0.02	7	0.18	-0.03	0.04	3	-0.03	0.01	3
HD 149890	6030	4.0	1.1	-0.20	0.05	33	0.03	6	0.17	0.00	0.04	3	0.07	0.07	3
HD 156617	5780	3.9	1.0	-0.03	0.04	33	0.03	7	0.08	-0.09	0.05	5	0.07	0.07	4
HD 156893	5300	3.8	0.9	-0.21	0.04	36	0.03	8	0.22	0.02	0.05	4	0.23	0.07	4
HD 157214	5640	4.0	0.8	-0.36	0.04	33	0.02	6	0.42	0.07	0.04	3	0.32	0.03	4
BD +40 3374	5050	4.6	0.8	-0.43	0.05	31	0.06	4	...	0.05	0.05	3	0.27	0.02	3
HD 171009	5840	4.0	1.0	-0.35	0.04	32	0.04	6	...	-0.01	0.04	3	0.19	0.04	3
HD 171242	5920	3.8	0.9	-0.22	0.06	22	0.05	6	0.22	0.05	0.01	3	0.21	0.04	3
HD 178478	5550	3.6	1.0	-0.50	0.03	24	0.04	5	0.40	0.11	0.02	3	0.35	0.04	4
HD 188326	5310	3.8	0.9	-0.18	0.05	35	0.04	6	0.21	0.05	0.06	3	0.22	0.05	4
HD 206373	5900	3.8	1.1	-0.16	0.04	26	0.02	5	0.15	0.06	0.03	3	0.09	0.08	4
HD 210483	5850	4.0	0.9	-0.04	0.04	29	0.06	4	...	-0.04	0.05	5	0.06	0.10	4
HD 211476	5840	4.2	0.9	-0.10	0.05	32	0.03	7	...	-0.03	0.02	3	0.01	0.03	4
HD 217511	6460	3.7	1.4	-0.12	0.03	20	0.05	6	0.30	0.06	0.03	2	...	...	...
HD 219175	6050	4.2	0.9	-0.24	0.05	30	0.03	5	...	-0.04	0.04	5	0.05	0.04	4
Thin-disc stars															
HD 115383	6090	4.0	1.2	0.20	0.05	29	0.05	8	0.02	0.00	0.01	4	0.08	0.07	3
HD 127334	5610	4.0	0.8	0.24	0.05	33	0.07	7	-0.15	0.01	0.06	5	0.08	0.11	4
HD 136064	6090	3.9	1.1	0.05	0.06	30	0.04	7	...	0.02	0.03	3	0.16	0.14	2
HD 163989	6240	3.7	1.3	0.06	0.04	30	0.03	8	0.16	0.04	0.07	3	0.24	0.14	3
HD 187013	6290	3.6	1.3	0.00	0.05	22	0.04	7	...	0.01	0.04	3	0.27	0.01	2
HD 187691	6140	3.9	1.2	0.20	0.05	35	0.05	8	0.02	0.01	0.02	5	0.22	0.09	3
HD 200790	6190	3.9	1.3	0.08	0.04	32	0.02	8	...	0.05	0.05	3	0.32	0.09	2
HD 220117	6480	3.4	1.2	0.22	0.04	23	0.04	6	...	...	...	...	...	...	...
Thick-disc stars															
HD 150433	5650	4.2	0.9	-0.34	0.05	37	0.05	7	...	0.07	0.01	3	0.31	0.04	4
HD 181047	5550	4.2	0.8	0.01	0.05	35	0.04	6	...	-0.02	0.02	5	0.06	0.05	3
HD 186411	5860	3.7	1.2	0.11	0.05	34	0.03	8	0.00	0.00	0.01	5	0.16	0.05	3
HD 195019	5750	4.0	0.9	0.11	0.03	37	0.04	8	0.10	-0.10	0.01	5	0.07	0.08	4
HD 198300	5830	4.1	0.9	-0.44	0.04	38	0.04	8	...	-0.03	0.03	3	0.11	0.05	4

Star	[Al/Fe]	σ	n	[Si/Fe]	σ	n	[Ca/Fe]	σ	n	[Sc/Fe]	σ	n	[TiI/Fe]	σ	n
Group 1 stars															
HD 3795	0.38	0.03	3	0.20	0.05	16	0.25	0.05	7	0.16	0.04	10	0.28	0.05	15
HD 4607	0.03	...	1	0.06	0.06	8	0.11	0.06	6	0.02	0.06	6	0.10	0.05	8
HD 15777	0.20	0.05	2	0.18	0.05	20	0.15	0.04	9	0.22	0.06	12	0.18	0.07	13
HD 22872	-0.05	0.04	3	0.03	0.05	19	-0.01	0.06	9	0.02	0.05	12	-0.02	0.05	14
HD 25123	0.03	0.01	2	0.00	0.04	20	0.00	0.05	11	0.04	0.04	10	0.02	0.05	18
HD 40040	0.26	0.01	3	0.16	0.05	19	0.21	0.06	11	0.21	0.05	12	0.30	0.06	17
HD 49409	0.04	0.06	2	0.05	0.04	15	0.13	0.04	10	0.10	0.05	10	0.16	0.05	12
HD 52711	-0.05	0.04	4	0.04	0.05	20	0.06	0.05	11	-0.01	0.05	12	0.02	0.05	18
HD 60779	0.01	0.04	2	0.04	0.05	19	0.07	0.05	8	0.01	0.05	11	0.07	0.05	15
HD 67088	-0.02	0.00	2	0.01	0.05	21	0.05	0.04	10	0.00	0.05	12	-0.04	0.05	16
HD 67587	0.11	0.06	3	0.09	0.05	16	0.14	0.05	9	0.05	0.05	8	0.10	0.05	13
HD 76095	0.18	0.01	2	0.08	0.05	21	0.09	0.05	10	0.07	0.04	10	0.08	0.05	18
HD 77408	0.04	0.04	3	0.01	0.06	14	0.05	0.04	7	0.08	0.05	9	0.11	0.05	8
HD 78558	0.27	0.05	3	0.22	0.05	18	0.22	0.05	9	0.14	0.05	12	0.29	0.05	16
HD 88371	0.25	0.03	3	0.16	0.05	20	0.22	0.06	11	0.22	0.05	9	0.27	0.05	24
HD 88446	0.06	0.04	3	0.09	0.05	20	0.12	0.05	9	0.06	0.05	12	0.14	0.06	10
HD 90508	0.16	0.04	3	0.10	0.05	21	0.14	0.04	11	0.05	0.04	11	0.13	0.05	18
HD 109498	0.06	0.03	3	0.03	0.06	14	0.01	0.06	7	0.02	0.02	8	0.02	0.06	7
HD 111367	0.07	0.05	4	0.03	0.04	20	0.04	0.04	10	0.04	0.04	11	0.05	0.05	14
HD 135694	0.19	0.02	3	0.07	0.06	11	0.12	0.06	7	0.03	0.04	8	0.07	0.06	6
HD 138750	-0.03	0.03	2	0.03	0.05	20	0.12	0.05	9	0.04	0.04	11	0.12	0.05	10
HD 140209	0.10	...	1	0.08	0.05	19	0.09	0.06	7	0.07	0.05	9	0.08	0.04	12
HD 149105	-0.01	0.03	2	-0.03	0.04	15	0.04	0.07	5	0.01	0.04	8	-0.01	0.05	7
HD 149890	0.00	0.04	3	0.01	0.05	18	0.01	0.04	7	-0.05	0.04	7	-0.02	0.05	6

Table .4. continued.

Star																	
HD 156617	0.06	0.04	4	-0.01	0.04	18	0.03	0.05	11	-0.02	0.04	10	0.03	0.05	15
HD 156893	0.29	0.04	3	0.14	0.04	20	0.16	0.05	11	0.18	0.05	11	0.19	0.05	25
HD 157214	0.31	0.05	2	0.22	0.04	16	0.22	0.06	8	0.15	0.04	9	0.26	0.04	12
BD +40 3374	0.38	0.03	3	0.20	0.05	18	0.23	0.04	8	0.24	0.04	8	0.38	0.07	22
HD 171009	0.12	...	1	0.12	0.04	15	0.15	0.06	7	0.13	0.04	7	0.19	0.03	8
HD 171242	0.01	0.04	2	0.10	0.05	11	0.14	0.04	7	0.02	0.05	7	0.11	0.04	10
HD 178478	0.33	0.04	3	0.20	0.05	14	0.25	0.05	7	0.06	0.06	7	0.31	0.06	8
HD 188326	0.22	0.00	2	0.13	0.03	15	0.12	0.05	7	0.07	0.05	6	0.20	0.05	13
HD 206373	0.02	0.03	4	0.04	0.05	15	0.05	0.02	6	0.04	0.04	8	0.05	0.03	7
HD 210483	0.07	0.03	3	0.00	0.05	17	0.05	0.06	7	0.02	0.04	8	0.04	0.05	18
HD 211476	0.05	0.01	2	-0.01	0.04	16	0.02	0.03	6	-0.03	0.04	8	0.01	0.03	9
HD 217511	0.00	0.04	2	0.03	0.05	17	0.06	0.05	9	0.10	0.05	7	0.02	0.05	6
HD 219175	-0.06	...	1	-0.01	0.06	15	0.01	0.05	7	-0.02	0.03	9	0.02	0.04	6
Thin-disc stars															
HD 115383	...	...	...	0.06	0.05	13	0.08	0.04	8	0.00	0.06	9	0.07	0.04	8
HD 127334	0.07	0.03	2	0.03	0.05	20	0.00	0.05	11	-0.02	0.05	10	-0.03	0.05	16
HD 136064	-0.04	0.03	2	0.00	0.05	15	0.09	0.05	6	0.10	0.04	8	-0.02	0.05	10
HD 163989	0.04	0.07	4	0.06	0.05	15	0.04	0.03	4	0.06	0.05	9	0.10	0.06	8
HD 187013	-0.04	0.02	2	0.06	0.06	11	0.09	0.04	4	0.01	0.06	7	0.09	0.06	5
HD 187691	0.00	0.06	3	0.03	0.05	18	0.05	0.02	8	0.01	0.05	12	0.03	0.05	12
HD 200790	0.01	0.01	2	0.04	0.05	16	0.01	0.04	7	0.05	0.05	9	0.00	0.04	7
HD 220117	0.01	...	1	0.00	0.05	9	0.10	0.05	5	0.06	0.04	4	0.12	0.05	6
Thick-disc stars															
HD 150433	0.10	...	1	0.17	0.05	18	0.22	0.05	9	0.19	0.05	9	0.28	0.05	18
HD 181047	0.05	0.02	2	0.03	0.04	20	0.05	0.05	11	-0.02	0.05	11	-0.01	0.05	23
HD 186411	0.05	0.02	3	0.00	0.05	20	0.11	0.04	8	0.02	0.04	9	0.03	0.05	18
HD 195019	-0.02	0.03	3	-0.01	0.04	20	0.02	0.05	10	-0.04	0.05	11	-0.02	0.05	25
HD 198300	0.18	0.05	4	0.03	0.03	19	0.03	0.05	9	-0.01	0.05	11	0.1	0.06	11

Star	[TiII/Fe]	σ	n	[V/Fe]	σ	n	[Cr/Fe]	σ	n	[Co/Fe]	σ	n	[Ni/Fe]	σ	n
Group 1 stars															
HD 3795	0.20	0.06	4	0.15	0.05	11	0.07	0.05	13	0.15	0.03	6	0.04	0.05	23
HD 4607	0.06	0.02	3	0.03	0.03	5	-0.01	0.06	13	-0.06	0.05	5	-0.04	0.05	15
HD 15777	0.22	0.03	4	0.12	0.05	8	0.02	0.05	17	0.12	0.05	8	0.00	0.05	27
HD 22872	-0.03	0.06	4	0.02	0.05	13	0.00	0.05	19	-0.05	0.05	10	-0.04	0.05	30
HD 25123	0.02	0.04	4	0.00	0.04	10	0.00	0.06	17	0.00	0.05	9	-0.02	0.06	30
HD 40040	0.26	0.04	4	0.14	0.06	12	0.03	0.06	17	0.11	0.05	6	0.04	0.04	28
HD 49409	0.08	0.02	4	0.14	0.05	10	0.02	0.05	14	0.03	0.03	7	-0.01	0.05	19
HD 52711	0.03	0.06	4	-0.02	0.05	12	0.01	0.05	18	-0.02	0.05	10	-0.02	0.05	29
HD 60779	0.03	0.05	4	0.06	0.06	9	0.01	0.06	15	-0.03	0.06	9	-0.02	0.05	28
HD 67088	-0.05	0.06	4	-0.06	0.06	14	0.00	0.05	19	-0.07	0.04	9	-0.05	0.05	29
HD 67587	0.06	0.02	4	0.13	0.05	6	0.03	0.06	14	0.06	0.04	5	-0.03	0.05	23
HD 76095	0.12	0.04	3	0.06	0.05	12	0.05	0.05	17	0.05	0.04	9	-0.02	0.05	30
HD 77408	0.10	0.07	3	0.07	0.05	5	-0.02	0.05	11	0.03	0.04	6	-0.05	0.05	14
HD 78558	0.20	0.05	4	0.07	0.05	12	0.04	0.06	18	0.08	0.04	8	0.02	0.05	28
HD 88371	0.27	0.02	4	0.13	0.04	14	0.04	0.06	18	0.07	0.03	10	0.04	0.05	28
HD 88446	0.04	0.02	4	0.02	0.03	5	0.00	0.05	14	0.04	0.02	5	-0.05	0.04	23
HD 90508	0.07	0.04	4	0.06	0.05	13	0.01	0.05	18	0.03	0.05	10	-0.02	0.05	30
HD 109498	0.01	0.03	4	0.00	0.04	6	0.01	0.07	15	0.01	0.03	4	-0.04	0.06	18
HD 111367	-0.01	0.04	4	0.01	0.06	7	-0.01	0.04	16	-0.02	0.05	8	-0.04	0.05	28
HD 135694	0.05	0.00	2	-0.03	0.05	9	0.02	0.04	12	0.01	0.03	6	-0.07	0.05	14
HD 138750	0.08	0.08	4	0.04	0.05	5	0.00	0.05	14	-0.02	0.05	6	-0.06	0.05	24
HD 140209	0.04	0.03	3	0.04	0.05	9	0.04	0.05	15	0.01	0.05	7	-0.03	0.06	26
HD 149105	-0.06	0.03	2	-0.08	0.01	3	-0.01	0.09	15	-0.08	0.06	5	-0.04	0.03	24
HD 149890	-0.01	0.02	3	-0.02	0.04	5	-0.02	0.07	13	-0.06	0.04	9	-0.07	0.05	21
HD 156617	-0.04	0.05	4	-0.05	0.04	12	0.02	0.05	17	-0.05	0.03	9	-0.07	0.05	29
HD 156893	0.17	0.05	4	0.08	0.05	14	0.02	0.06	16	0.05	0.04	11	0.00	0.05	27
HD 157214	0.10	0.01	2	0.13	0.03	5	0.02	0.08	12	0.16	0.03	5	0.03	0.06	19
BD +40 3374	0.30	0.04	3	0.24	0.04	7	0.10	0.05	13	0.19	0.04	8	0.04	0.06	24
HD 171009	0.11	0.04	3	0.07	0.04	4	-0.02	0.08	13	0.06	0.08	5	-0.03	0.05	16
HD 171242	0.03	0.05	4	0.03	0.04	8	0.03	0.04	12	0.05	0.05	4	-0.09	0.05	15
HD 178478	0.21	0.01	3	0.16	0.05	8	0.10	0.06	9	0.07	0.03	4	-0.03	0.05	18
HD 188326	0.27	0.03	4	0.14	0.06	9	0.05	0.05	15	0.10	0.04	7	0.02	0.05	21
HD 206373	0.03	0.05	4	0.01	0.05	5	-0.04	0.05	13	-0.03	0.04	4	-0.04	0.04	18
HD 210483	0.01	0.04	4	-0.06	0.02	7	0.01	0.07	14	-0.04	0.05	9	-0.06	0.05	26
HD 211476	0.00	0.04	4	-0.03	0.04	6	0.01	0.05	16	-0.04	0.04	7	-0.04	0.04	22
HD 217511	0.06	0.01	2	...	...	...	0.00	0.05	8	0.04	0.01	4	-0.01	0.05	13
HD 219175	-0.03	0.03	3	-0.02	0.05	8	-0.05	0.05	9	-0.04	0.03	3	-0.08	0.05	22
Thin-disc stars															
HD 115383	0.07	0.03	3	0.00	0.06	7	0.02	0.06	16	0.02	0.05	5	-0.01	0.04	20
HD 127334	-0.07	0.04	4	-0.03	0.05	13	0.03	0.05	15	0.02	0.04	8	0.02	0.05	26
HD 136064	0.05	0.03	3	0.01	0.05	8	0.03	0.05	12	-0.04	0.03	6	-0.04	0.05	16
HD 163989	0.08	0.03	4	0.02	0.08	4	-0.03	0.05	11	-0.03	0.05	6	-0.07	0.05	23
HD 187013	0.09	0.01	2	...	...	...	0.02	0.06	9	...	...	...	-0.04	0.05	13
HD 187691	0.02	0.03	4	-0.04	0.05	7	0.00	0.04	17	-0.07	0.06	6	-0.03	0.05	28
HD 200790	-0.04	0.03	4	-0.04	0.05	5	0.01	0.04	15	-0.04	0.05	6	-0.03	0.04	23
HD 220117	...	...	...	...	...	...	0.00	0.06	7	...	...	...	-0.04	0.04	9
Thick-disc stars															
HD 150433	0.26	0.03	2	0.17	0.05	8	0.07	0.05	16	0.07	0.05	7	0.04	0.05	25
HD 181047	-0.05	0.05	4	-0.02	0.05	14	0.05	0.06	18	-0.02	0.06	11	-0.01	0.05	26
HD 186411	0.02	0.03	4	-0.01	0.06	12	0.01	0.06	17	-0.04	0.05	7	-0.07	0.05	27
HD 195019	-0.05	0.05	4	-0.05	0.05	12	0.01	0.05	19	-0.05	0.05	8	-0.06	0.05	30
HD 198300	0.03	0.05	4	0.01	0.04	7	-0.04	0.06	16	0.04	0.02	6	-0.06	0.05	26

Table .5. Elemental abundances of neutron-capture elements for programme and comparison stars.

Star	[Y/Fe]	σ	n	[ZrI/Fe]	σ	n	[ZrII/Fe]	σ	n	[Ba/Fe]	[La/Fe]	σ	n
Group 1 stars													
HD 3795	-0.03	0.03	6	0.17	0.07	4	0.08	0.02	2	-0.06	0.20	0.05	3
HD 4607	-0.02	0.02	5	0.07	0.02	3	0.07	0.01	2	0.28	-0.05	0.07	2
HD 15777	-0.13	0.06	4	0.13	0.00	3	0.10	0.09	2	-0.14	-0.01	0.01	3
HD 22872	-0.12	0.01	6	-0.06	0.08	4	-0.01	0.09	2	0.00	-0.16	0.05	3
HD 25123	-0.07	0.05	7	0.07	0.02	2	-0.04	0.01	2	0.06	0.00	0.04	4
HD 40040	-0.22	0.03	4	0.03	0.01	2	-0.05	0.05	2	-0.13	0.02	0.06	2
HD 49409	-0.21	0.08	2	0.19	0.05	2	0.11	...	1	0.07	-0.13	...	1
HD 52711	-0.16	0.03	7	0.08	0.05	5	0.05	0.04	2	-0.08	-0.06	0.06	4
HD 60779	-0.06	0.06	7	0.05	0.03	3	0.01	0.04	2	0.11	-0.04	0.06	4
HD 67088	-0.20	0.04	7	-0.20	0.03	3	-0.15	0.04	2	0.00	-0.03	0.05	4
HD 67587	-0.16	0.05	4	-0.10	...	1	-0.18	...	1	0.08	0.01	0.00	3
HD 76095	-0.05	0.06	5	0.00	0.05	3	0.00	0.04	2	0.24	0.14	0.01	2
HD 77408	-0.08	0.01	3	...	...	...	0.17	...	1	0.21	0.07	...	1
HD 78558	-0.13	0.05	6	0.07	0.09	2	-0.01	0.01	2	-0.13	-0.16	0.04	2
HD 88371	0.03	0.07	4	0.06	0.03	4	0.06	0.02	2	-0.18	-0.09	...	1
HD 88446	0.57	0.05	5	0.57	...	1	0.56	0.01	2	1.04	0.70	0.08	4
HD 90508	-0.19	0.05	6	-0.06	0.05	4	-0.01	0.01	2	-0.05	0.02	0.04	3
HD 109498	-0.09	0.02	6	-0.02	0.06	3	-0.03	0.04	2	-0.07	-0.01	0.07	2
HD 111367	-0.17	0.05	6	0.00	0.06	3	-0.02	0.03	2	0.06	0.06	0.05	2
HD 135694	-0.20	0.07	3	-0.01	0.07	4	0.01	...	1	-0.04	...	...	...
HD 138750	0.00	0.04	7	0.16	0.03	3	0.04	0.07	2	0.19	0.04	0.05	4
HD 140209	-0.13	0.03	4	0.00	0.04	3	-0.14	0.06	2	-0.24	-0.07	0.02	3
HD 149105	-0.16	0.04	5	-0.02	...	1	-0.03	0.01	2	0.11	-0.07	0.00	2
HD 149890	-0.15	0.04	6	0.09	...	1	0.07	...	1	0.00	-0.02	0.01	2
HD 156617	-0.21	0.05	6	-0.09	0.04	2	-0.07	...	1	0.03	-0.07	0.08	3
HD 156893	-0.03	0.06	6	-0.02	0.04	6	0.04	0.02	2	0.21	0.15	0.07	3
HD 157214	-0.13	0.07	5	0.08	0.06	4	0.05	0.03	2	-0.26	-0.06	0.06	2
BD +40 3374	-0.14	0.07	3	0.30	0.04	5	0.34	...	1	...	0.04	...	1
HD 171009	-0.12	0.04	4	0.17	0.03	3	0.09	...	1	0.02	0.05	0.05	3
HD 171242	-0.14	0.00	2	0.24	...	1	0.21	0.06	2	...	0.20	0.01	2
HD 178478	-0.15	0.10	3	0.18	0.04	2	...	...	...	-0.24	0.11	0.05	3
HD 188326	-0.05	0.06	5	0.06	0.03	6	0.02	...	1	0.00	0.13	0.05	3
HD 206373	-0.09	0.06	6	...	...	...	-0.14	...	1	0.16	-0.07	0.05	3
HD 210483	-0.17	0.05	4	0.00	0.02	2	-0.05	0.02	2	-0.11	-0.03	0.06	3
HD 211476	-0.16	0.06	7	-0.04	0.04	5	0.00	0.06	2	-0.10	0.06	0.05	2
HD 217511	0.11	0.02	5	...	...	...	...	...	...	...	0.21	0.01	2
HD 219175	-0.15	0.04	5	-0.09	...	1	-0.09	0.00	2	0.00	0.12	0.00	2
Thin-disc stars													
HD 115383	-0.17	0.06	5	0.00	...	1	-0.03	0.05	2	-0.05	-0.09	...	1
HD 127334	-0.20	0.05	6	-0.15	0.05	7	-0.15	0.03	2	...	-0.17	0.06	3
HD 136064	0.05	0.00	2	...	...	...	0.19	0.04	2	0.05	0.08	...	1
HD 163989	0.01	0.05	5	...	...	...	0.03	0.01	2	0.03	0.08	0.09	3
HD 187013	-0.15	0.03	5	-0.12	...	1	-0.12	...	1	0.00	0.07	0.04	2
HD 187691	-0.13	0.07	6	-0.10	...	1	-0.09	0.01	2	-0.14	-0.05	0.02	3
HD 200790	-0.18	0.04	5	-0.12	...	1	-0.11	0.07	2	-0.17	-0.07	0.05	4
HD 220117	...	...	...	...	...	...	...	...	...	-0.17	...	...	...
Thick-disc stars													
HD 150433	-0.06	0.04	5	0.12	0.06	4	0.12	...	1	-0.16	0.00	0.04	2
HD 181047	0.00	0.06	7	-0.08	0.05	4	-0.05	0.01	2	-0.01	-0.06	0.02	3
HD 186411	-0.05	0.05	6	-0.03	0.04	3	-0.03	0.04	2	0.04	0.03	0.06	4
HD 195019	-0.17	0.06	7	-0.20	0.04	4	-0.17	0.04	2	-0.01	-0.09	0.06	4
HD 198300	-0.14	0.06	5	-0.02	0.09	2	...	...	...	0.05	-0.01	0.07	3

Star	[Ce/Fe]	σ	n	[Pr/Fe]	σ	n	[Nd/Fe]	σ	n	[Sm/Fe]	σ	n	[Eu/Fe]	σ	n
Group 1 stars															
HD 3795	0.17	0.06	2	0.44	0.14	2	0.32	0.03	6	0.44	0.13	3	0.64	0.03	2
HD 4607	-0.02	0.00	2	0.14	...	1	0.08	0.04	4	0.11	0.01	2	0.03	0.04	2
HD 15777	0.04	0.02	3	0.14	0.05	2	0.12	0.05	5	0.18	0.05	3	0.30	0.04	2
HD 22872	-0.09	0.09	3	0.02	0.06	2	-0.10	0.02	7	-0.01	0.08	3	-0.07	0.06	2
HD 25123	-0.08	0.05	5	-0.05	0.01	2	-0.06	0.05	5	-0.06	0.04	3	-0.04	0.00	2
HD 40040	-0.05	0.06	3	0.24	0.02	2	0.09	0.05	5	0.21	0.05	2	0.28	0.03	2
HD 49409	-0.04	0.06	2	0.23	...	1	0.25	0.03	3	0.24	0.07	3	0.33	...	1
HD 52711	-0.09	0.05	4	-0.01	0.12	2	-0.04	0.05	5	-0.01	0.03	3	-0.08	0.04	2
HD 60779	0.03	0.04	3	0.19	...	1	-0.02	0.07	6	0.01	0.03	3	0.01	0.02	2
HD 67088	-0.10	0.03	4	0.06	0.03	2	-0.08	0.05	6	-0.03	0.06	3	-0.01	0.08	2
HD 67587	-0.06	0.05	2	...	...	...	0.07	0.07	3	...	...	...	0.02	0.06	2
HD 76095	0.13	0.04	4	0.16	0.06	2	0.16	0.07	7	0.15	0.01	2	0.22	0.04	2
HD 77408	0.06	...	1	0.21	...	1	0.20	0.02	3	0.22	...	1	0.16	0.02	2
HD 78558	-0.02	0.05	5	0.22	0.03	2	0.03	0.05	5	0.16	0.01	2	0.20	0.01	2
HD 88371	0.00	0.04	3	0.11	...	1	0.08	0.03	5	0.21	0.01	3	0.24	...	1
HD 88446	0.65	0.03	4	0.56	0.06	2	0.66	0.03	7	0.55	0.06	2	0.34	0.09	2
HD 90508	-0.08	0.09	3	0.11	0.07	2	0.06	0.04	8	0.18	0.03	3	0.17	0.01	2
HD 109498	0.08	0.03	4	0.17	0.04	2	0.08	0.06	4	0.15	0.00	2	0.16	0.05	2
HD 111367	0.09	...	1	0.14	0.00	2	-0.04	0.07	4	0.06	0.00	2	0.02	0.06	2
HD 135694	0.01	0.08	3	0.26	...	1	0.00	0.05	4	0.21	0.08	3	0.23	0.11	2
HD 138750	0.03	0.08	3	0.12	0.07	2	0.04	0.04	5	0.04	0.05	3	0.01	0.01	2
HD 140209	-0.04	0.03	5	0.08	...	1	0.00	0.03	5	0.05	0.04	3	0.09	0.04	2
HD 149105	-0.09	0.02	2	-0.1	...	1	0.02	0.03	4	0.10	0.11	2	0.08	0.05	2
HD 149890	-0.03	...	1	-0.02	...	1	-0.02	0.02	4	0.07	...	1	0.02	0.00	2
HD 156617	-0.07	0.02	4	-0.13	0.04	2	-0.06	0.04	5	-0.01	0.02	3	-0.02	0.05	2

Table .5. continued.

HD 156893	0.04	0.09	3	0.26	0.08	2	0.20	0.02	8	0.34	0.01	2	0.38	0.02	2
HD 157214	-0.08	0.03	3	0.13	0.01	2	0.04	0.06	5	0.27	0.05	3	0.28	0.02	2
BD +40 3374	0.19	0.05	3	...	...	...	0.30	0.06	3	0.29	0.05	3	0.51	0.01	2
HD 171009	0.05	0.09	3	0.27	...	1	0.12	0.06	6	0.25	0.06	2	0.29	0.03	2
HD 171242	0.20	0.07	2	...	...	...	0.14	0.04	5	0.36	...	1	0.24	...	1
HD 178478	-0.04	0.05	2	...	...	...	-0.04	0.04	4	...	...	...	0.19	0.07	2
HD 188326	0.09	0.05	3	0.19	0.01	2	0.13	0.04	7	0.19	0.05	3	0.21	0.04	2
HD 206373	-0.02	0.05	3	0.2	0.00	2	-0.03	0.05	3	-0.02	0.03	2	-0.01	...	1
HD 210483	-0.10	0.09	4	0	...	1	-0.03	0.04	6	-0.04	...	1	-0.02	...	1
HD 211476	-0.10	0.06	4	0.11	...	1	0.02	0.05	5	0.09	0.07	3	0.05	0.02	2
HD 217511	0.14	...	1	...	...	...	0.20	...	1	0.16	...	1	0.14	0.01	2
HD 219175	-0.04	0.06	2	0.14	...	1	-0.03	0.06	4	0.04	0.00	2	0.05	0.01	2
Thin-disc stars															
HD 115383	-0.19	0.01	2	0.03	...	1	-0.13	0.03	4	-0.15	0.03	3	-0.09	0.01	2
HD 127334	-0.20	0.03	4	-0.14	...	1	-0.17	0.05	6	-0.21	0.04	2	-0.19	0.06	2
HD 136064	...	...	...	0.10	...	1	0.05	0.07	4	...	...	...	0.09	0.06	2
HD 163989	0.08	0.03	3	0.03	...	1	0.04	0.03	3	0.06	0.05	2	-0.01	0.04	2
HD 187013	-0.04	...	1	-0.05	0.01	2	-0.17	0.03	2	-0.08	0.08	2	-0.11	0.03	2
HD 187691	-0.16	0.05	3	-0.10	...	2	-0.22	0.04	4	-0.05	...	1	-0.07	0.00	2
HD 200790	-0.09	0.08	4	-0.19	0.03	2	-0.16	0.05	5	-0.09	0.02	2	-0.15	0.00	2
HD 220117	...	...	...	...	...	...	...	...	...	...	...	...	...	...	...
Thick-disc stars															
HD 150433	-0.08	...	1	0.37	...	1	0.12	0.03	4	0.34	...	1	0.25	0.03	2
HD 181047	-0.02	0.05	3	0.07	...	1	-0.02	0.04	6	0.07	0.06	2	0.01	0.08	2
HD 186411	-0.11	0.05	4	-0.06	0.13	2	-0.05	0.04	6	-0.06	0.02	2	-0.03	0.01	2
HD 195019	-0.10	0.02	4	-0.01	0.06	2	-0.06	0.04	8	-0.01	0.08	3	-0.03	0.08	2
HD 198300	-0.03	0.07	4	0.28	0.06	2	0.07	0.02	3	0.25	0.01	2	0.12	0.00	2